REPUBLIQUE ALGERIENNE DEMOCRATIQUE ET POPULAIRE

Ministry of Higher Education and Scientific Research

National Polytechnic School

Mechanical engineering department

Final Year Project memory

For obtaining the diploma of state engineer in Mechanical Engineering

---

Numerical modeling of a fluid temperature during drilling operations

---

Sofiane KOUZRITE

Under the direction of	M. Said	RECHAK	Professor
	M. Abdelouaheb	BOUGHELOUM	Engineer at SONATRACH

Presented and publicly defended on 07 September 2020

Composition of the Jury:

President	M. Arezki SMAILI	Professor	ENP
Promoter	M. Said RECHAK	Professor	ENP
Co-promoter	M. Abdelouaheb BOUGHELOUM	Expert Engineer	Sonatrach
Examiner	M. Imene KHEBOURI	PhD student	ENP

ENP 2020

REPUBLIQUE ALGERIENNE DEMOCRATIQUE ET POPULAIRE

Ministry of Higher Education and Scientific Research

National Polytechnic School

Mechanical engineering department

PFE project

For obtaining the diploma of state engineer in Mechanical Engineering

Numerical modeling of a fluid temperature during drilling operations

Sofiane KOUZRITE

Under the direction of	M. Said	RECHAK	Professor
	M. Abdelouaheb	BOUGHELOUM	Engineer at SONATRACH

Presented and publicly defended on 07 September 2020

Composition of the Jury:

President	M. Arezki SMAILI	Professor	ENP
Promoter	M. Said RECHAK	Professor	ENP
Co-promoter	M. Abdelouaheb BOUGHELOUM	Expert Engineer	Sonatrach
Examiner	M. Imene KHEBOURI	PhD student	ENP

ENP 2020

ملخص

يعد الحصول على معلومات دقيقة حول درجة حرارة سوائل الحفر عملية حاسمة عند التخطيط لعمليات الحفر. الهدف من هذه المذكرة هو تطوير نموذج يمكن أن يحسب توزيع درجة حرارة الآبار.

يتم اشتقاق نموذج درجة الحرارة بناءً على توازن الطاقة بين التكوين و البئر, في هذه المذكرة ، يتم تحسين توازن الطاقة من خلال تنفيذ توليد الحرارة,و من خلال مراعاة اعتماد خصائص سوائل الحفر مثل اللزوجة والكثافة على درجة الحرارة والضغط.كما تم إدخال تدرج حراري غير خطي كدالة لميل حفرة البئر لتوسيع النموذج ليشمل الآبار غير العمودية.

.يرتبط المجال الرئيسي لتطبيق هذا النموذج بتحسين تصميم سائل الحفر ، مما يؤدي في النهاية إلى عمليات حفر آمنة ومربحة

الكلمات الدالة: نموذج درجة الحرارة ، سوائل الحفر، الحفر

Résumé

Le but de ce PFE est de développer un code sous le MATLAB environnement "Well-temp". Ce code est basé sur un algorithme qui prend en considération les paramètres réels du forage comme les sources d'énergie et la dépendance de la densité et de la viscosité sur la température et la pression. Le modèle de température est validé, puis une l'analyse de sensibilité est présentée. Un gradient géothermique non linéaire en fonction de l'inclinaison du puits de forage est également introduit pour étendre le modèle aux puits de forage déviés. Le domaine principal d'application de ce modèle est lié à l'optimisation des paramètres de conception du fluide de forage, ce qui conduit finalement à des opérations de forage rentables.

Mots-clés: Modèle de température, les fluides non newtonien, forage

Abstract

Having accurate information about the temperature of drilling fluids is a critical process when planning drilling operations. Hence, one of main parts of the PFE project is to develop a computer code under MATLAB environment "Well-temp". This code is based on an algorithm which takes into account on the real parameters of the drilling such as the energy sources and the dependence of the density and the viscosity on the temperature and on the pressure. The implemented temperature model is firstly validated, then a sensitivity analysis is secondly conducted.

A nonlinear geothermal gradient as a function of the inclination of the wellbore is also introduced to extend the model to deviated wellbores. The main area of application of this model is related to the optimization of the design parameters of the drilling fluid, which ultimately leads to safe and profitable drilling operations.

Keywords: Temperature model, non-Newtonian fluids, drilling

Acknowledgements

I want to thank everyone who supported and helped me in developing and writing this PFE.

First of all, allow me to thank my promoters Mr S.RECHAK and Mr A.BOUGHELOUM. For their patience, their availability and above all their sound advice throughout the development and the writing of this thesis.

I also thank all of the professors in the mechanical engineering department of the National Polytechnic School responsibles for my training, who consistently and pedagogically provided me with the tools necessary for the success of my engineering studies in mechanical engineering.

I would like to express my gratitude to the members of the jury, Mr Arezki SMAILI who did me the honor of chairing this jury and Ms Imene KHEBOURI who was kind enough to judge my work.

How can I end these thanks without mentioning my parents and friends who have shown constant support, and encouragement to me.

Dedications

I dedicate this modest work

To my parents who supported and encouraged me during all my years of study

May they find here the testimony of my deep gratitude

To my family who warmly supported and encouraged me throughout my course

To all my friends to whom I wish much success

Table of Contents

List of Tables

List of Figures

Nomenclature

Chapter 01: Introduction, Literature review, problematic 13

Introduction 14

Literature review 14

Problematic 15

Thesis structure 15

Chapter 02: Wellbore heat transfer theory 16

Introduction 17

2.1. Wellbore heat transfer 17

2.2. Transport and thermophysical properties of drilling fluid 18

2.2.1. Convective heat transfer coefficient 18

2.2.2. Temperature and Pressure Dependent Rheological Parameters 20

2.3. Energy source terms 25

Drill pipe rotation 25

Drill bit friction 26

Frictional pressure losses 27

Joule-Thomson effect 27

Conclusion 28

Chapter 03: Temperature and pressure distributions 29

Introduction 30

3.1. Derivation of the heat transfer equations 30

The differential equation for the drill pipe temperature 30

The differential equation for the annulus temperature 31

Solution 32

3.2. Inlet mud temperature models 33
3.2.1. Constant Inlet mud temperature 33
3.2.2. Variable Inlet mud temperature 33
3.3. Pressure calculation 36
Annular flow 36
Pipe flow 38
Conclusion 39
Chapter 04: Presentation of "WELL-TEMP" code. 40
Introduction 41
4.1. Numerical approach 41
4.2. Algorithm 43
4.3. Shooting method 46
4.4. "WELL – TEMP" architecture 48
Inputs 48
Output 49
4.5. Model Validation 50
Conclusion 52
Chapter 05: Results and discussions 53
Introduction 54
5.1. Flow rate 54
5.2. Specific heat capacity 56
5.3. Thermal conductivity 58
Drilling fluid 58
Formation 60
Drill pipe 62
5.5. Drilling fluid density 64
5.6. Geothermal gradient 66

5.7. Energy source terms 68
Joule Thomson coefficient 68
Frictional pressure losses 69
5.8. Effect of pressure and temperature on density and viscosity on temperature 70
..... 71
5.9. Circulation Time 72
5.10. Multi layers well 72
Conclusion 75
General conclusion 77
References 78
Appendix 80
Swift and Holmes model [13] 81
Basic Assumptions and Equations 81
Solution of Equations to Derive Circulating Mud Temperatures 82
Hasan and Kabir's Model [14] 83

List of tables:

Table 2. 1 Various forced convection correlations for circular tubes 20
Table 2. 2 density of solids in drilling fluids..... 22
Table 2. 3 coefficients for oil density correlation..... 22
Table 2. 4 coefficients for eauqtion 1.17..... 23
Table 4. 1 well and mud circulating properties 50
Table 5. 1 dimensions of the multi layers well..... 75

List of figures

Fig 2.1 Wellbore schematic 17
Fig 2.2 drilling fluid density 24
Fig 3.1 wellbore element 30
Fig 3.2 Schematic representation of the heat-transfer model 33
Fig 4.1 discretized wellbore 41
Fig 4.2 Intermediate Value Theorem 47
Fig 4.3 some inputs of the model 49
Fig 4.4 Comparison of steady state temperature distribution of 3 methods with the same heat transfer coefficients 51
Fig 4.5 Comparison of steady state temperature distribution of 3 methods with adjusted heat transfer coefficients 52
Fig 5. 1 Temperature distribution - flow rate: 500 l/min 55
Fig 5. 2 Temperature distribution - flow rate: 2000 l/min 55
Fig 5. 3 Temperature vs. flow rate 56
Fig 5. 4 Temperature distribution - specific heat capacity: 1000 J/kg-°C 57
Fig 5. 5 Temperature distribution - specific heat capacity: 2000 J/kg-°C 57
Fig 5. 6 Temperature vs. specific heat capacity 58
Fig 5. 7 Temperature distribution - thermal conductivity: 1 W/m-°C 59
Fig 5. 8 Temperature distribution - thermal conductivity: 2 W/m-°C 59
Fig 5. 9 Temperature vs. drilling fluid thermal conductivity 60
Fig 5. 10 Temperature distribution – formation thermal conductivity: 1.75 W/m-°C 61
Fig 5. 11 Temperature distribution – formation thermal conductivity: 3 W/m-°C 61
Fig 5. 12 Temperature vs. formation thermal conductivity 62
Fig 5. 13 Temperature distribution – drill pipe thermal conductivity: 80 W/m-°C 63
Fig 5. 14 Temperature distribution – drill pipe thermal conductivity: 30 W/m-°C 63
Fig 5. 15 Temperature vs. drill pipe thermal conductivity 64
Fig 5. 16 Temperature distribution – density: 1700 kg/m^3 65
Fig 5. 17 Temperature distribution – density: 1000 kg/m^3 65
Fig 5. 18 Temperature vs. drilling fluid density 66
Fig 5. 19 Temperature distribution – geothermal gradient: 13.15 °C/km 67
Fig 5. 20 Temperature vs. geothermal gradient 68

Fig 5. 21 Temperature distribution – geothermal gradient: 33.15 °C/km 67
Fig 5. 22 Bottom hole temperature vs. flow rate 69
Fig 5. 23 Bottom hole temperature vs. flow rate 70
Fig 5. 24 flow rate of 300 l/min 71
Fig 5. 25 flow rate of 3000 l/min 71
Fig 5. 26 temperature vs circulation time 72
Fig 5. 27 multi layers wellbore schematic 73
Fig 5. 28 compariason between a multi layer well and an open hole well 74

Nomenclature

c_p	Specific heat capacity	$J/kg°C$
k	Conductivity	$W/m.°C$
ρ	Density	kg/m^3
v	Velocity	m/s
μ	Viscosity	$Pa.s$
h	Convective heat transfer coefficient	$W/m^2°C$
Q	Flow rate	m^3/s
q''	Heat flux	W/m^2
r	Radius	m
T	Temperature	$°C$
U	Overall heat transfer coefficient	$W/m^2°C$
t	Circulation time	s
α	Formation heat diffusivity	m^2/s
P	pressure	Pa
G	Geothermal gradient	°C/m
m	Masse rate	kg/s
x	Measured depth	m
ϕ	Energy source term	J/s
dx	Box length	m
I	Angle of inclination	deg
n	Number of boxes	-
F	Axial force	N
L	Length	m
N_r	Rotary pipe speed	1/min
RPS	Rotations per second	1/s
v_h	Axial pipe velocity	m/s

v_r	Tangential pipe speed	m/s
w	Unit pipe weight	N/m
α	Angle of inclination	rad
β	Buoyancy factor	-
θ	Dogleg angle	radians
μ	Friction factor	-
τ_q	Torque	N.m
ϕ	Azimuth	rad
ψ	Angle between axial and tangential pipe velocities	rad

Subscripts

a	Annulus
p	Pipe
w	Wellbore
wb	Wellbore
f	Formation
i	Inner
o	Outer
c	Casing
D	Dimensionless

Chapter 01: Introduction, Literature review, problematic

Introduction

The drilling operation is carried out by a tool driven by a rotational movement which, by rolling over the rocks, breaks them up. On the surface of the ground, the drilling equipment consists of the drilling rig and the packing, the drilling rig is the visible part, it includes a tower, on which are placed the lifting equipment that allows handling, screwing and unscrewing the rods and changing the tool, the drill string is the not visible and the active part. In well planning the key to achieving objectives successfully is to design drilling programs on the basis of anticipation of potential problems, drilling problems can be very costly, the most prevalent drilling problems include Pipe sticking, pipe failure, dog legs and telescopic holes, key seats in holes, shale problems, lost circulation problems.

During drilling, fluid is circulated through the drill pipe/annulus system and this fluid circulation process serves several fundamental functions: removal of the large amount of drilled cuttings from the wellbore, prevention of breakdown of the wellbore by adjusting the mud weight and circulation rate, thus controlling the pressure, cooling and lubricating of the drill bit.

Drilling fluid cools down the formation around the hole. As the depth of the well increases, so does the temperature due to the geothermal gradient of the earth. This process may heat the fluid to dangerous temperatures and cause a problem.

Literature review

Many authors have worked on the drilling over the years from the sixties to this day to ensure a safe drilling operations and to solve the problems that occur during drilling operations such as the "Stick-slip" phenomenon and the effect of high temperatures and high pressures on the drilling fluid such as the work of HOLMES and SWIFT 1970 and the work of HASAN and KABIR 1996.

The National Polytechnic School ENP has worked in callaboration with the SONATRACH development center in this recent years, projects have been carried out in different themes such as "Analysis and modeling of buckling in drill strings" made by Mr. Seif Eddine BELOUAHED and Mr. Kheireddine BOUGHACHICHE and the subject of "Modeling of torsion vibrations in drill strings" carried out by M.Mohamed El Amine KOURTA and Mr.Okba SAFSAF, and a third project with the theme "modeling of the coupling of vibrations in drill strings in a wellbore" by Ms. Yamina Dounya SAHLI.

This year a project on the prediction of the temperature of a fluid during drilling operations has been proposed and we will try to give everything to solve the problem and to better contribute to the development of the Algerian industry and university.

Problematic

The main part of the PFE project is to develop a computer code under the MATLAB environment "WELL-TEMP". This code is based on an algorithm which takes into account on the real parameters of the drilling such as the energy sources and the dependence of the density and the viscosity on the temperature and on the pressure. The implemented temperature model is firstly validated, then a sensitivity analysis is secondly conducted.

Thesis structure

The present memory is structured as follow. Chapter 1 presents the introduction, consisting of the literature review, research problem. Chapter 2 takes us through the different modes of heat transfer present in the wellbore, how to calculate the overall heat transfer coefficient for a given wellbore configuration, the correlations used in this work for the calculation of the convective heat transfer coefficient, the calculation of the thermo-physical properties such as the density and the viscosity models, and the energy source terms that occur during drilling. Chapter 3 contains the derivation of the temperature model, its solution, and its validation, and the calculation of the pressure. In Chapter 4, the computer code "Well-temp" is presented. We present the Implementation of the model into "Well-temp". All the explanations on how the "Well-temp" works are given from the inputs up to the outputs. The analysis of the results obtained via "Well-temp" is presented in Chapter 5 Appendix presents two analytical models that we used for the validation of our model; these are the models of KABIR and HOLMES.

Chapter 02: Wellbore heat transfer theory

Introduction

Heat transfer can be defined as thermal energy in transit due to a spatial temperature difference to temperature differences [1]. In this chapter, heat transfer theory in wellbore is presented starting by explaining the different modes of heat transfer in the well such as convection, correlations for the calculation of the convective heat transfer coefficient are introduced, the models needed for the temperature model such as the density and the viscosity models and the energy sources models are also presented in this chapter.

2.1. Wellbore heat transfer

During drilling operations, temperature differences between the wellbore and the formation result in a transfer of thermal energy.

Figure 2.1 represents a schematic of a wellbore and it's divided into 3 zones they will help us to explain the heat transfer in the wellbore.

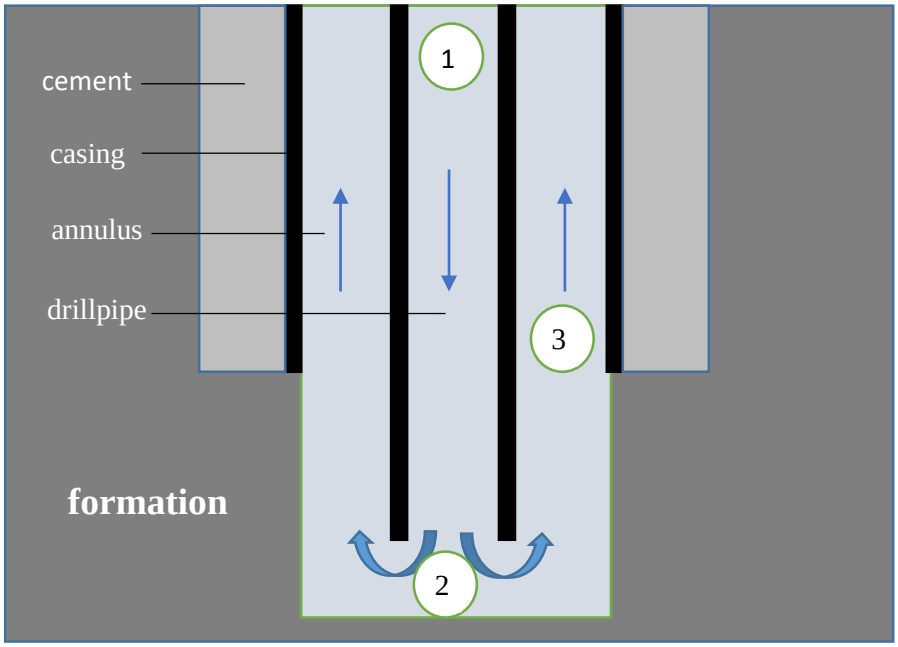

Fig 2. 1 Wellbore schematic

Starting with the first zone which is the drill pipe, as the drilling fluid flows down through the drill pipe its temperature will change due to heat transfer processes, we site; the convection between the fluid column and between the fluid, the drill pipe wall, and the annular fluid and heat generation from the fluid friction.

The second zone represents the drill bit, it's considered as a single point. Heat is generated at this point from frictional forces between the bit and the formation during drilling.

After the drilling fluid passes through the bit, it enters the third zone which is the annulus and its temperature will be affected by the convection between the fluid column and between the fluid, the drill pipe wall, the drill pipe fluid and also between the fluid, the casing, the formation and the heat generation from fluid friction

The wellbore temperature distribution is affected by the formation temperature and it's also sensitive to wellbore design and drilling parameters.

[2] Presented a solution for the formation heat loss by including Fourier's law of heat conduction as a boundary condition for the formation/wellbore interface. The algebraic solution is given by:

$$T_D = 1.1281\sqrt{t_D}(1 - 0.3\sqrt{t_D}) \text{ for } t_D \leq 1.5 \qquad (2.1)$$

$$T_D = [0.4036 + 0.5\ln(t_D)]\left[1 + \frac{0.6}{t_D}\right] \text{ for } t_D > 1.5 \qquad (2.2)$$

Where

$$t_D = \frac{\alpha t}{r_{wb}^2}$$

And

$$\alpha = \frac{k_f}{c_{pf}\rho_f}$$

Here, T_D represents the dimensionless temperature and t_D represents the dimensionless. The dimensionless temperature gives the transient behavior of the formation temperature.

2.2. Transport and thermophysical properties of drilling fluid

2.2.1. Convective heat transfer coefficient

Convection is defined as the heat transfer that occurs between a surface and a moving fluid at different temperatures [1].

The expression for the convective heat transfer process is given by Newton's law of cooling:

$$q'' = h(T_s - T_m) \qquad (2.3)$$

Where h is the convective heat transfer coefficient (CHTC), and T_s and T_m represent the temperature of the conduit surface and the mean temperature of the fluid, respectively.

In chapter 2.1, the heat transfer processes that occur in a wellbore are presented. It was mentioned that a convective heat transfer between the drill pipe fluid, the drill pipe wall, and the annulus fluid exists. The same process occurs between the annulus fluid, the casing wall and a possible cement layer, and the

formation. Instead of applying equation (2.3) to describe these processes individually, an overall heat transfer coefficient that considers the net resistance of heat flow over several layers, is used. The convective heat transfer is modeled by the following equations [3]:

$$Q_{ap} = 2\pi r_{pi} U_p (T_a - T_p) dx \qquad (2.4)$$

$$Q_{wa} = 2\pi r_{ci} U_a (T_w - T_a) dx \qquad (2.5)$$

Where Q_{ap} and Q_{wa} represents the overall rate of heat transfer from the annulus to the drill pipe and from the formation/wellbore interface to the annulus, respectively. The overall heat transfer coefficient is defined by [4] as:

$$\frac{1}{U_p} = \frac{1}{h_p} + \frac{r_{pi}}{r_{po}}\frac{1}{h_a} + \frac{r_{pi}}{k_p}\ln\left(\frac{r_{po}}{r_{pi}}\right) \qquad (2.6)$$

$$\frac{1}{U_a} = \frac{1}{h_a} + \frac{r_{ci}}{k_c}\ln\left(\frac{r_{co}}{r_{ci}}\right) + \frac{r_{ci}}{k_{cement}}\ln\left(\frac{r_w}{r_{co}}\right) \qquad (2.7)$$

For equation (2.7), it is possible to include additional casing strings and cement layers.

The CHTC is determined by the dimensionless Nusselt number given below:

$$Nu = \frac{hD}{k} \qquad (2.8)$$

Where $D = 2.r_{pi}$ in pipe flow

And $D = r_{po}.\ln\left(\frac{r_{ci}}{r_{po}}\right)$ in annulus flow

The Nusselt number gives a relationship between the convective and the conductive heat transfer, and a large Nusselt number indicates an efficient convection process.

The most common CHTC correlations for forced convection in circular tubes are presented in Table 2.1, [5], for both turbulent and laminar flow regimes.

Table 2.1 Various forced convection correlations for circular tubes

	Forced convection correlation	Parameter and flow conditions
Turbulent flow	$Nu = 0.023Re^{\frac{4}{5}}.Pr^{n}$	$0.7 \leq Pr \leq 160$ $10000 \leq Re$ $\frac{L}{D} \geq 10$
	$Nu = 0.027Re^{\frac{4}{5}}.Pr^{\frac{1}{3}}\left(\frac{\mu}{\mu_s}\right)^{0.14}$	$0.7 \leq Pr \leq 16700$ $Re \geq 5.10^{6}$ $\frac{L}{D} \geq 10$
	$Nu = \frac{(f/8)(Re-1000)Pr}{1.07 + 12.7\left(\frac{f}{8}\right)^{0.5}(Pr^{\frac{2}{3}}-1)}$	$f = (0.79\ln Re - 1.64)^{-2}$ $6000 \leq Re \leq 5.10^{6}$ $0.5 \leq Pr \leq 2000$
	$St = 0.071Re^{-0.33}Pr^{0.67}$	$Nu = St.Pe$ $Pe = Re.Pr$
Transient flow	$Nu = 0.116\left(Re^{\frac{2}{3}} - 125\right)Pr^{\frac{1}{3}}\left(1 + \left(\frac{d}{L}\right)^{\frac{2}{3}}\right)$	$2300 \leq Re \leq 6000$
Laminar flow	$Nu = 4.36$	$Re \leq 2300$

Where

$$Re = \frac{\rho v D}{\mu} \qquad (2.9)$$

Here D represents the hydraulic diameter (m)

$D = 2r_{pi}$ for pipe flow

$D = 2(r_{ci} - r_{po})$ for the annulus flow

And

$$Pr = \frac{\mu c_p}{k} \qquad (2.10)$$

2.2.2. Temperature and Pressure Dependent Rheological Parameters

Density model

Drilling mud is composed of four major components: water or brine phase, an oil phase, low density solids, and high density solids. These four components are immiscible; no component dissolves in any other

component to any significant degree. This means that the four components form an ideal mixture. In an ideal mixture, the sum of the component volumes equals the total volume of the mixture:

$$V_f = V_w + V_o + V_{ls} + V_{hs} \qquad (2.11)$$

where V_f is the total fluid volume, V_w is the volume of the water phase, V_o is the volume of the oil phase, V_{ls} is the volume of the low density solids, and V_{hs} is the volume of the high density solids.

The total weight of a fluid mixture is simply the sum of the weights of the components. Conservation of mass ensures that the total weight calculation is always correct:

$$m_f = \rho_w V_w + \rho_o V_o + \rho_{ls} V_{ls} + \rho_{hs} V_{hs} \qquad (2.12)$$

Where m_f is the mass of the fluid mixture, ρ_w is the density of the water phase, ρ_o is the density of the oil phase, ρ_{ls} is the density of the low-density solids, and ρ_{hs} is the density of the high-density solids. The overall density of the fluid mixture, then, is

$$\rho_f = \frac{m_f}{V_f} = \frac{\rho_w V_w}{V_f} + \frac{\rho_o V_o}{V_f} + \frac{\rho_{ls} V_{ls}}{V_f} + \frac{\rho_{hs}}{V_f}$$

$$= \rho_w f_w + \rho_o f_o + \rho_{ls} f_{ls} + \rho_{hs} f_{hs} \qquad (2.13)$$

Where f_w is the volume fraction of the water phase, f_o is the volume fraction of the oil phase, f_{ls} is the volume fraction of the low density solids, and f_{hs} is the volume fraction of the high density solids. Note that the sum of the volume fractions equals 1. The specific gravities of typical drilling fluid solids are given in Table 2.2. Changes in temperature and pressure will change the volumes of the components. While the solid phases show little change over typical ranges of temperature and pressure, water does show some change with temperature, and oil shows considerable change with pressure and temperature. Water is relatively incompressible, while oils are much more compressible. If we review Eq. 2.12, we see that the volume of the fluid changes as the volume of the water phase and oil phase changes. As a result, the volume fractions, computed at a given pressure and temperature, are not constants and vary with changes in pressure and temperature. If we measure volume fractions at a specified temperature, the following formula gives the density of the mixture at new temperatures and pressures:

$$\rho_f(P,T) = \frac{\rho_f(P_r,T_r)}{1 - \frac{f_o \Delta\rho_o}{\rho_o(P,T)} - \frac{f_w \Delta\rho_w}{\rho_w(P,T)}} \qquad (2.14)$$

Where

$$\Delta\rho_w = \rho_w(P,T) - \rho_w(P_r,T_r)$$

$$\Delta\rho_o = \rho_o(P,T) - \rho_o(P_r,T_r)$$

Where P_r is the reference temperature and T_r is the reference temperature used to calculate the volume fractions f_w and f_o.

Water and Oil Densities.

For a precise analytical formula of water density, we recommend the following correlation:

$$\rho_w = 8.63186 - 3.31977 \times 10^{-3}T + 2.37170 \times 10^{-5}P \qquad (2.15)$$

Where ρ_w is the density of water in lbm/gal, T is the temperature in °F and P is the pressure in psi.

A general correlation for the density of oil is given by:

$$\rho_o = 8.3154 \times \{(a_0T + b_0) + (a_1T + b_1)P + (a_2T + b\_2)P^2\} \qquad (2.16)$$

Where ρ_o is the density of oil in lbm/gal, T is the temperature in °F and P is the pressure in psi, Table 2.3. gives the values of the coefficients for diesel and four synthetic oils.

Table 2. 2 density of solids in drilling fluids

Bentonile	2.6	Limestone	2.8	Hematite	5.05	Galena	7.5
Barite	4.2	Siderite	3.08	Ilmetite	4.6	Cuttings	2.6
Attapulgite	2.89	Sand	2.63	NaCl	2.16	$CaCl_2$	1.96

Table 2. 3 coefficients for oil density correlation

	$a_0 \times 10^4$	$b_0 \times 10$	$a_1 \times 10^8$	$b_1 \times 10^{16}$	$a_2 \times 10^{13}$	$b_2 \times 10^{12}$
Diesel	-3.6058	8.7071	0.4640	3.6031	-1.6843	-72.465
LVT 200	-3.8503	8.3847	1.5695	2.4817	-4.3373	6.5076
LAO C16C18	-3.5547	8.1304	1.2965	3.1227	-2.7166	-28.894
Saraline 200	-3.7621	8.0019	1.5814	2.3560	-4.3235	10.891
EMO-4000	-3.7799	8.4174	1.3525	2.8808	-3.1847	-17.697

PVT model

In order to avoid the repetition of all the stages explained previously one can use a correlation for the calculation of the density of the drilling fluid at any temperature and pressure. The correlation is linear in temperature and quadratic in pressure and it takes the following form:

$$\rho_f = (A_0T + B_0) + (A_1T + B_1)P + (A_2T + B_2)P^2 \qquad (2.17)$$

Example:

The studied fluid is an oil base type with 100% Diesel, and Barite as the high density solids without water nor low density solids, we use this drilling fluid for all the simulations to come.

Intervals for temperature and pressure are chosen so that it is ensured that the temperatures and pressures calculated do not exceed the limits of these two intervals; and practically we can choose:

The range of temperatures is set from 50 to 300 °F.

The range of pressures is set from 0 to 18000 psi.

The reference temperature and pressure are: $P_r = 0\ psi \qquad T_r = 60\ °F$

The density of the drilling fluid at the reference temperature and pressure ($0\ psi, 60\ °F$) is 2500 kg/m^3

After calculating the drilling fluid density using equation 1.14, we can interpolate the results to find the coefficients $A_{i=0,1,2}$ and $B_{i=0.1.2}$ in equation 1.16.the results are presented in table 2.4

Figure 2.2 shows a comparison between the densities calculated by equation 2.13 which are represented by stars and the densities of the interpolation (equation 1.17) the maximum difference between the two densities is $1.9 \times 10^{-4} kg/l$. We can now use equation 1.16 for the rest of the calculations without returning to the density model represented by equation 2.13 and this will allow us to reduce the execution time and to simplify the model.

Table 2. 4 coefficients for equation 2.17

A_0	-4.59×10^{-04}	B_0	1.226
A_1	$6..38 \times 10^{-09}$	B_1	4.49×10^{-06}
A_2	-2.26×10^{-13}	B_2	-9.07×10^{-11}

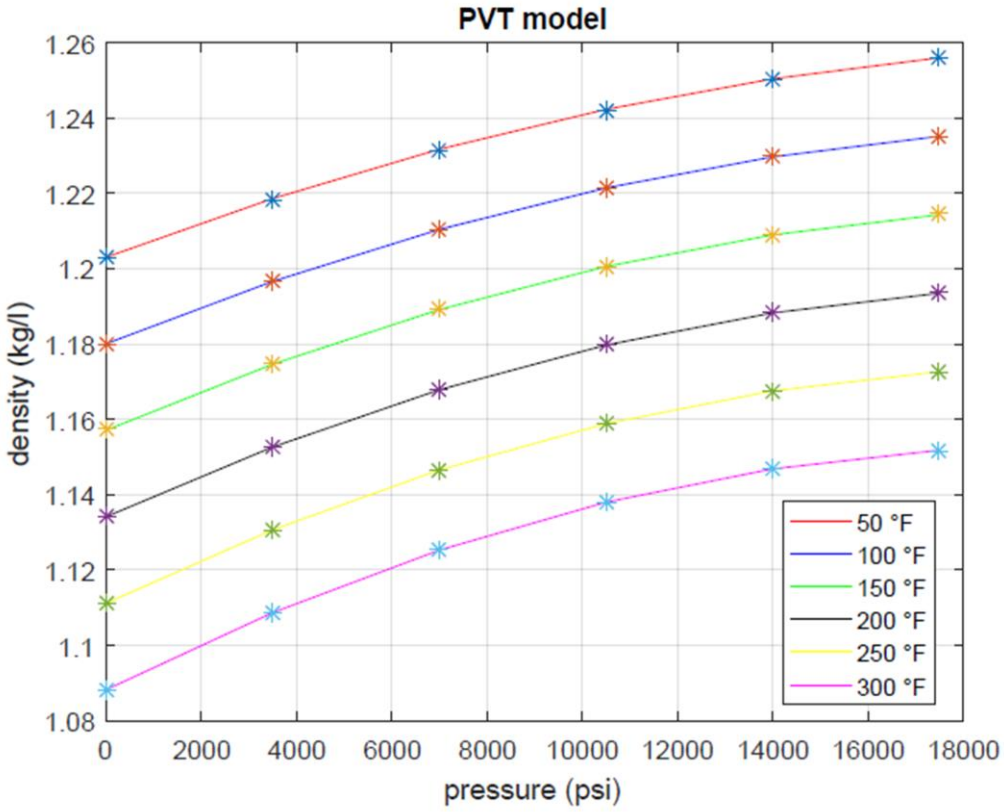

Fig 2. 2 drilling fluid density

Power law model

A power-law fluid, is a type of generalized non Newtonian fluid for which the shear stress, τ, is given for most common drilling fluids by:

$$\tau = K\dot{\gamma}^{n} \qquad (2.18)$$

K is a measure of the consistency of the fluid, the higher the value of *k* the more viscous the fluid is; *n* is a measure of the degree of non-Newtonian behavior of the fluid. In cases where the flow behavior index is equal to 1, the power law model describes the behavior of a Newtonian fluid. In situations where the flow behavior index is between 0 and 1, the fluid is referred to as pseudo-plastic.

Viscosity model

The viscosity is a very weak function of pressure, so that its relation with temperature can be expressed as [6]

$$\mu(T) = \bar{\mu}\left(\frac{T}{70}\right)^{a+b\left(\frac{T}{70}\right)} \qquad (2.19)$$

Where T is the temperature in °F and the constant are a=-1.163, b=0 for oil and a=-1, b=-0.04 for water.

The apparent viscosity $\bar{\mu}$ is calculated from the power low model (see pressure calculation in chapter 3).

2.3. Energy source terms

To provide a more realistic temperature model, the following energy source terms are implemented in this work

1. Drill pipe rotation
2. Drill bit friction
3. Frictional pressure losses
4. Joule-Thomson coefficient

Drill pipe rotation

In a deviated wellbore, the drill pipe tends to lay at the low side of the wellbore. Consequently, friction occurs at the drill pipe and casing/formation interface and heat is generated during rotation. To quantify the amount of heat that is generated because of wellbore friction, the following equation is applied [7]:

$$q_p = \tau_q \times 2\pi \times RPS \qquad (2.20)$$

where q_p is regarded as the heat rate or down hole power loss, τ_q is the torque acting on the drill pipe due to wellbore friction and RPS represents the drill pipe rotations per second.

The torque is calculated by a 3D wellbore friction model given by [8]. This model gives an analytical solution of torque and drag that applies for straight sections, build-up-bends, drop-off-bends, side bends, and any combination of these situations

Straight sections

For a straight section, the torque acting on the drill pipe is expressed as

$$\tau_q = \pi r \beta w \Delta L . \sin\alpha . \cos\psi \qquad (2.21)$$

Curved sections

For any type of bend, the axial force in the drill pipe is determined by

$$F_2 = F_1 + F_1\left(e^{\pm|\theta_1-\theta_1|} - 1\right)\sin\psi + \beta w \Delta L\left[\frac{\sin\alpha_2 - \sin\alpha_1}{\alpha_2 - \alpha_1}\right] \qquad (2.22)$$

Where $+$ indicates tripping out and $-$ indicates tripping in. The parameters F_2 and F_1 refers to the axial force at the top and the bottom of a drill pipe element of the length ΔL. Since this is a 3D model, the

absolute change of direction is considered by implementing the dogleg. The dogleg may be determined from the equation below.

$$\cos\theta = \sin\alpha_1 \sin\alpha_2 \cos(\phi_1 - \phi_2) + \cos\alpha_1 \cos\alpha_2 \qquad (2.23)$$

Here, the subscripts 1 and 2 represent two successive survey measurements. Finally, the torque for a curved section is determined by equation (2.24).

$$\tau_q = \mu F_1 |\theta_1 - \theta_1| \cos\psi \qquad (2.24)$$

For all the equations above, ψ represents the angle between the axial and tangential pipe velocities during combined motion. The parameter is obtained from the following relationship:

$$\psi = \tan^{-1}\left(\frac{v_h}{v_r}\right) = \tan^{-1}\left(\frac{60v_h}{2\pi N_r r}\right) \qquad (2.25)$$

More details regarding the derivation of the model and corresponding theory is found in [8].

Drill bit friction

When the drill bit works on the formation to crush the rock, friction occurs at the interface of the bit and the formation and heat is generated.

The effect of frictional heating from the bit have a significant impact on the temperature distribution, it will be an advantage to have an idea of which parameters to adjust to control the heat generation. Mechanical specific energy (MSE) is a term commonly utilized as a measure of drilling efficiency. The term gives the energy required to remove a unit volume of rock. MSE is defined by:

$$MSE = \frac{total\ energy\ input}{volume\ removed} \qquad (2.26)$$

The expression can also be given as [9]

$$MSE = \frac{WOB}{Area} + \frac{2\pi.RPM.\tau_b}{Area.ROP} \qquad (2.27)$$

We can manipulate the operational parameters in equation (2.27) to minimize the MSE.

The heat generated from penetrating the rock can be estimated as

$$q_b = \tau_b 2\pi.RPS + \lambda.ROP.WOB \qquad (2.28)$$

WOB is the weight on bit, RPM is the rotation per minute, Area is the wellbore area, τ_b is the torque bit and ROP is the rate of penetration.

Frictional pressure losses

The third source of heat occurs as drilling fluids are circulated through the drill pipe and the annulus. Whenever a fluid flows through a pipe, a velocity gradient is present in the fluid. The velocity gradient appears because the fluid in contact with the pipe surface has zero velocity according to the no-slip condition. The heat due to the friction of the fluid in circulation is given as [10]

$$q_l = \Delta P \times Area \times v \qquad (2.29)$$

Joule-Thomson effect

As a liquid or a gas is either compressed or expanded, a subsequent change of temperature is experienced. To consider this effect in the temperature model, the Joule-Thomson (JT) coefficient is implemented. The JT coefficient is given by [10]

$$\mu_{jt} = \frac{1}{c_p}\left\{T\left[\frac{\partial}{\partial T}\left(\frac{1}{\rho}\right)\right]_P - \frac{1}{\rho}\right\} \qquad (2.30)$$

By introducing the density model given in (2.17), the equation becomes

$$\mu_{jt} = \frac{1}{c_p}\left\{-\frac{(B_2 + 2A_2T)P^2 + (B_1 + 2A_1T)P + B_0 + 2A_0T}{(B_0 + B_2P^2 + B_1P + A_0T + A_1PT + A_2P^2T)^2}\right\} \qquad (2.31)$$

The heat due to the JT effect can be finally expressed as

$$q_{JT} = mc_p\mu_{jt}\frac{\Delta P}{\Delta x} \qquad (2.32)$$

Where m is the mass rate. The JT coefficient may take a positive or negative sign. The point at which the sign changes is referred to as the inversion point. A negative sign indicates that the drilling fluid will heat as it expands and cool as it compresses.

In summary, the total amount of energy for fluids in drill pipe is

$$\phi_p = q_l - q_{JT} \qquad (2.33)$$

And the total amount of energy for fluids in annulus is then given as

$$\phi_a = q_l + q_{JT} + q_b + q_p \qquad (2.34)$$

Conclusion

The first step in establishing the temperature model is completed in this chapter. It is one of the most important steps. With the understanding of the heat transfer phenomenon in wells along with the necessary definitions of models such as the density, and the viscosity, and the energy sources models we will be able to move on to the mathematical development of the temperature model.

Chapter 03: Temperature and pressure distributions

Introduction

In this chapter, the mathematical model that governs the heat transfer processes during a drilling operation is presented. Due to the complexity of the problem, analytical models are not very efficient to obtain the exact temperature distribution, unless if simplifications are included due to the required hypothesis. The model includes computations of the pressure distribution and some inlet mud temperature models.

3.1. Derivation of the heat transfer equations

A derivation of the developed temperature model is presented below

Figure 3.1 represents a general wellbore element at which the derivation is based on.

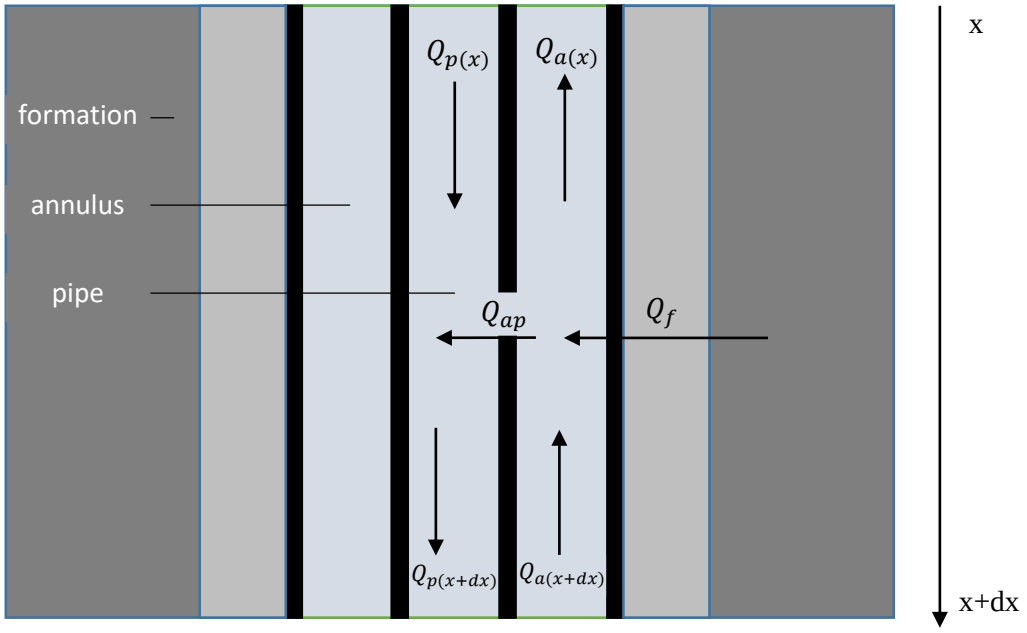

Fig 3. 1 wellbore element

The differential equation for the drill pipe temperature

In the drill pipe, the flow direction is set downwards and heat will therefore enter the system at x and leave the system at $x+dx$. Heat will also enter the system due to heat transfer with the annulus and heat generation from additional energy sources within the drill pipe.

The energy balance for the wellbore element is expressed by:

$$Q_{p(x+dx)} - Q_{p(x)} = Q_{ap} + \phi_p \qquad (3.1)$$

Where Q_{ap} represents the rate of heat transfer with the annulus and ϕ_p represents the energy sources present

$$Q_{p(x+dx)} - Q_{p(x)} = m_p\, c_{pp}\left(T_{p(x+dx)} - T_{p(x)}\right) \qquad (3.2)$$

Where $$T_{p(x+dx)} = T_{p(x)} + \frac{dT_p}{dx}dx \qquad (3.3)$$

$$Q_{p(x+dx)} - Q_{p(x)} = m_p\, c_{pp}\frac{dT_p}{dx}dx \qquad (3.4)$$

While the heat transfer across the drill pipe is expressed as [10]

$$Q_{ap} = 2\pi r_{pi} U_p\left(T_a - T_p\right)dx \qquad (3.5)$$

Where $r_{pi}$the inner radius of the drill pipe and U_p represents the overall heat transfer as explained in chapter 2.Combining equations (3.1-3.5) gives the following differential equation for the drill pipe temperature distribution:

$$\frac{dT_p}{dx} = A\left(T_a - T_p\right) + \frac{1}{m_p\, c_{pp}}\frac{\phi_p}{dx} \qquad (3.6)$$

Where

$$A = \frac{2\pi r_{pi} U_p}{m_p c_{pp}} \qquad (3.7)$$

The differential equation for the annulus temperature

For the annulus, the flow direction is set upwards and heat will consequently enter the system at x+dx and leave the system at x. Additional heat enters the system by heat transfer from the formation and heat generation due to energy sources in the annulus, and heat will also leave the system through the interface with the drill pipe.

The energy balance for the wellbore element becomes:

$$Q_{a(x+dx)} - Q_{a(x)} = Q_{ap} - Q_f - \phi_a \qquad (3.8)$$

Where Q_f gives the heat transfer from the formation to the wellbore interface and ϕ_a represents the energy sources in the annulus. Following [1], the thermal energy over the annulus element may be expressed by:

$$Q_{a(x+dx)} - Q_{a(x)} = m_a c_{pa}\left(T_{a(x+dx)} - T_{a(x)}\right) \qquad (3.9)$$

Where $$T_{a(x+dx)} = T_{a(x)} + \frac{dT_a}{dx}dx \qquad (3.10)$$

$$Q_{a(x+dx)} - Q_{a(x)} = m_a\, c_{pa}\frac{dT_a}{dx}dx \qquad (3.11)$$

The heat flow from the formation to the wellbore is given in the equation below [10].

$$Q_f = \frac{2\pi k_f}{T_D}(T_f - T_w)dx \qquad (3.12)$$

Here, T_w is the temperature at the interface between the formation and the wellbore. An approximation for the dimensionless temperature T_D is determined by the equations given in chapter 2. The heat transfer from the wellbore/formation interface to the annulus is given in equation (3.13).

$$Q_{wa} = 2\pi r_{ci} U_a (T_w - T_a)dx \qquad (3.13)$$

To eliminate T_w, we combine equations (3.12) and (3.13), the heat flow from the formation to the annulus is expressed by:

$$Q_f = \frac{2\pi r_{ci} U_a k_f}{k_f + r_{ci} U_a T_D}(T_f - T_a)dx \qquad (3.14)$$

Updating the energy balance in equation (3.8) with the expressions in equations (3.5), (3.11) and (3.14) yields the differential equation for the annulus temperature distribution as shown below.

$$\frac{dT_a}{dx} = C(T_a - T_p) - B(T_f - T_a) - \frac{1}{m_a c_{pa}}\frac{\phi_a}{dx} \qquad (3.15)$$

Where

$$C = \frac{2\pi r_{pi} U_p}{m_a c_{pa}} \qquad (3.16)$$

$$B = \frac{2\pi r_{ci} U_a k_f}{(k_f + r_{ci} U_a T_D) m_a c_{pa}} \qquad (3.17)$$

Solution

Considering equations (3.6) and (3.15), there is a set of two equations and two unknowns, explicitly T_p and T_a .to take the derivation further, equation (3.6) is rearranged to the following form:

$$T_a = \frac{1}{A}\frac{dT_p}{dx} + T_p - \frac{1}{A}\frac{1}{m_p c_{pp}}\frac{\phi_p}{dx} \qquad (3.18)$$

Substituting T_a in equation (3.15) with the expression above and solving for T_p gives

$$\frac{d^2T_p}{dx^2} - D\frac{dT_p}{dx} - ABT_p = -ABT_f - \frac{B+C}{m_p c_{pp}}\frac{\phi_p}{dx} - \frac{A}{m_a c_{pa}}\frac{\phi_a}{dx} \qquad (3.19)$$

Where

$$D = -A + B + C \qquad (3.20)$$

The differential equation in (3.19) is solved by the Undetermined Coefficients method. This method requires that the coefficients A, B, and C are constants. On the contrary, these coefficients are not constant throughout the wellbore because they involve the overall heat transfer coefficient. The overall heat transfer coefficient contains temperature dependent parameters such as drilling fluid density and viscosity and neither A, B, or C can be regarded as constants for the whole length of the wellbore. An analytical solution is consequently not achievable and hence numerical approaches are more suitable, object of the next chapter.

3.2. Inlet mud temperature models

3.2.1. Constant Inlet mud temperature

In this first model which is the most common, the inlet mud temperature is considered to be constant in time; where the user can chose one inlet mud temperature.

3.2.2. Variable Inlet mud temperature

In both this two models the inlet mud temperature is not constant in time.

Free convection with ambient air

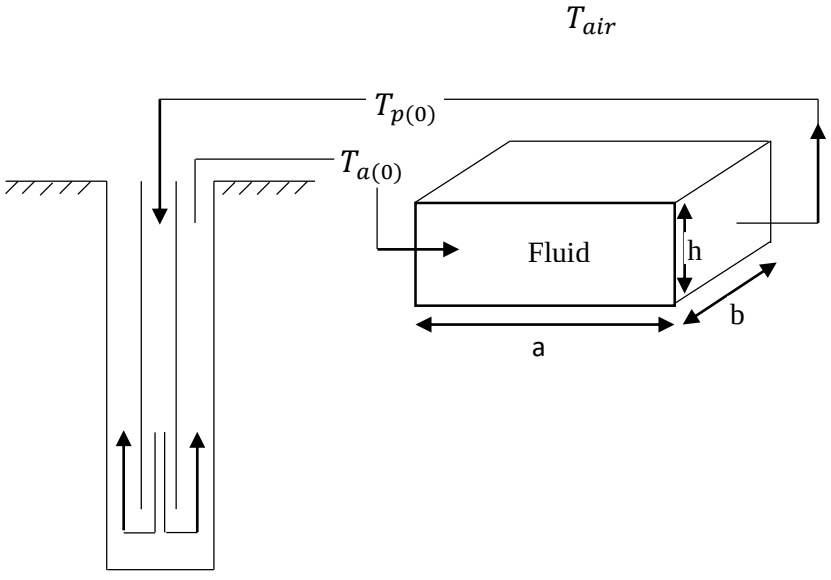

Fig 3.2 Schematic representation of the heat-transfer model

The fluid exiting the wellbore and entering the tank is at a temperature higher than the average value. Adding this hotter fluid gradually raises the tank fluid temperature with time. In other words, the wellbore acts as a heat exchanger supplying heat to the tank from the formation. However, as the tank temperature increases so does the heat loss from it to the surrounding air. The tank temperature finally approaches a steady value when the heat gained from the circulating fluid (from the formation) equals the heat lost to the ambient air.

Consider the case of forward circulation through a rectangular tank, as shown in Figure. 3.2. The energy is added to the tank by the fluid entering the tank at a temperature $T_{a(0)}$ (annulus fluid exit temperature), the energy is lost from the tank by the fluid exiting the tank (and entering the wellbore) at a temperature $T_{p(0)}$, and the heat is also lost from the tank to the ambient air.

The transient energy balance for the tank is given by [11]:

$$mc_p\left(T_{a(0)} - T_{p(0)}\right) - Uab\left(T_{p(0)} - T_{air}\right) = abh\rho c_p \frac{\partial T_{p(0)}}{\partial t} \qquad (3.21)$$

Rearranging

$$\frac{\partial T_{p(0)}}{\partial t} + \Omega T_{p(0)} = Y \qquad (3.22)$$

Where

$$\Omega = \frac{m + (Uab/c_p)}{abh\rho} \qquad (3.23)$$

$$Y = \frac{mT_{a(0)} + (UabT_{air}/c_p)}{abh\rho} \qquad (3.24)$$

Equation 3.24 is a linear differential equation and has the following solution

$$T_{p(0)} = \frac{Y}{\Omega} + Ce^{-\Omega t} \qquad (3.25)$$

The integration constant, C, is evaluated from the boundary condition ($T_{p(0)} = T_o$ at $t = 0$), giving the following solution

$$T_{p(0)} = \frac{Y}{\Omega} + (T_o - \frac{Y}{\Omega})e^{-\Omega t} \qquad (3.26)$$

Notice that in the equation. 3.26, we assumed that Y is a constant although it contains a term with $T_{a(0)}$. As the tank temperature increases, the exit fluid temperature from the annulus $T_{a(0)}$ would also increase

gradually with time. However, assuming $T_{a(0)}$ being constant is still reasonable because its variation with time is small. In addition, the term $mT_{a(0)}$ is generally much smaller than the term $UabT_{air}/c_p$.

Another interesting aspect of equation 3.26 is that the constant $\frac{Y}{\Omega}$ may be expressed as

$$\frac{Y}{\Omega} = \frac{mT_{a(0)} + (UabT_{air}/c_p)}{m + Uab} \qquad (3.27)$$

In many cases, the first term is much larger than the second, both in the numerator and denominator, Thus we can simplify equation 3.27 to yield

$$\frac{Y}{\Omega} = \frac{mT_{a(0)}}{m} = T_{a(0)} \qquad (3.28)$$

Combining equations 3.26 and 3.28 yields

$$T_{p(0)} = T_{a(0)} + (T_o - T_{a(0)})e^{-\Omega t} \qquad (3.29)$$

The calculus of U is given in [1]:

U in this case is equal to h the CHTC and considering the case of a forced convection in an external flow with a flat plate we can calculate h using correlations from [1].

The effect of variable properties of air may be considered by evaluating all properties at the film temperature

$$T = \frac{T_{air} + T_0}{2}$$

McQuillan and Culham [12] Provide an analytical formulas instead of using tables for evaluating the properties of air as follow:

$$\rho = \frac{351.99}{T} + \frac{344.84}{T^2} \qquad (3.30)$$

$$\mu = \frac{1.4592T^{3/2}}{109.10 + T} \qquad (3.31)$$

$$k = \frac{2.3340 \times 10^{-3}T^{\frac{3}{2}}}{164.54 + T} \qquad (3.32)$$

$$c_p = 1030.5 - 0.19975T + 3.9734 \times 10^{-4}T^2 \qquad (3.33)$$

From [1] :

$$\overline{Nu} = 0.664 Re^{1/2} Pr^{1/3} \text{ for } Pr > 0.6 \text{ and } Re < 5.10^5 \qquad (3.34)$$

$$\overline{Nu} = \left(0.037 Re^{4/5} - 871\right) Pr^{1/3} \text{ for } Pr > 0.6 \text{ and } 5.10^5 \leq Re \leq 10^8 \qquad (3.35)$$

Comments:

- Equation 3.29 shows that the tank fluid temperature approaches the final fluid exit temperature asymptotically.
- The parameters that are likely to have the largest effect are the initial tank temperature, the area of the tank exposed to the air (heat transfer area = ab), the heat transfer coefficient between the tank and the air (which could change dramatically with wind velocity), and the tank volume.

Constant difference between inlet and outlet mud temperatures

In some models a constant difference between inlet and outlet mud temperatures is maintained in other words

$$T_{a(0)} - T_{p(0)} = constant \qquad (3.36)$$

3.3. Pressure calculation

Annular flow

Flow section

$$S_{a(i)} = \pi(r_{ci(i)}^2 - r_{po(i)}^2) \qquad (3.37)$$

Annulus flow velosity

$$v_{a(i)} = \frac{Q}{S_{a(i)}} \qquad (3.38)$$

Hydraulic diameter

$$D_{ha(i)} = 2(r_{ci(i)} - r_{po(i)}) \qquad (3.39)$$

Effective diameter

$$D_{ea(i)} = \frac{3nD_{ha(i)}}{2n+1} \qquad (3.40)$$

Apparent viscosity

$$\mu_{aa(i)} = \left\{(0.4788 \times K)\left[\frac{12v_{a(i)}}{D_{ea(i)}}\right]^{n-1}\right\} \qquad (3.41)$$

Reynolds number

$$Re_{a(i)} = \frac{(D_{ea(i)})(\rho_{a(i)})(v_{a(i)})}{\mu_{aa(i)}} \qquad (3.42)$$

Hydrostatic pressure

$$P_{ha(i)} = \rho_{a(i)} g(x_i - x_{i-1}) + P_{ha(i-1)} \qquad (3.43)$$

$P_{ha(0)}$ is known and we can set it for exemple equals to 0 Pa

Reynolds number at Laminar flow boundary

$$Re_{lam} = 3470 - 1370 \times n \qquad (3.44)$$

Reynolds number at turbulent flow boundary

$$Re_{tur} = 4270 - 1370 \times n \qquad (3.45)$$

Friction factor

$$a = \frac{\log_{10}(n) + 3.93}{50} \qquad (3.46)$$

$$b = \frac{1.75 - \log_{10}(n)}{7} \qquad (3.47)$$

$$f_{a(i)} = \frac{24}{Re_{a(i)}} \text{ for } Re_{a(i)} < Re_{lam} \qquad (3.48)$$

$$f_{a(i)} = \left(\frac{24}{Re_{lam}}\right) + \left(\frac{Re_{a(i)} - Re_{lam}}{800}\right) \times \left(\left(\frac{\mathrm{a}}{Re_{tur}^{\mathrm{b}}}\right) - \left(\frac{24}{Re_{lam}}\right)\right) \text{ for } Re_{lam} \leq Re_{a(i)} \leq Re_{tur} \qquad (3.49)$$

$$f_{a(i)} = \frac{a}{Re_{a(i)}^{b}} \text{ for } Re_{a(i)} > Re_{tur} \qquad (3.50)$$

Pressure loss

$$\Delta P_{a(i)} = \left(\frac{f_{a(i)}(\rho_{a(i)})(v_{a(i)})^2}{2D_{ha(i)}}\right)(x_i - x_{i-1}) \qquad (3.51)$$

Cumulative pressure loss

$$PL_{cum,a(0)} = \Delta P_{a(0)} \qquad (3.52)$$

$$PL_{cum,a(i)} = PL_{cum,a(i-1)} + \Delta P_{a(i)} \qquad (3.53)$$

Dynamic pressure

$$P_{da(i)} = P_{ha(i)} + PL_{cum,a(i)} \qquad (3.54)$$

Pipe flow

Flow section

$$S_{p(i)} = \pi r_{pi(i)}^2 \qquad (3.41) \qquad (3.55)$$

Pipe flow velosity

$$v_{p(i)} = \frac{Q}{S_{p(i)}} \qquad (3.56)$$

Hydraulic diameter

$$D_{hp(i)} = 2r_{pi(i)} \qquad (3.57)$$

Effective diameter

$$D_{ep(i)} = \frac{4nD_{hp(i)}}{3n+1} \qquad (3.58)$$

Apparent viscosity

$$\mu_{ap(i)} = \left\{(0.4788 \times K)\left[\frac{8v_{p(i)}}{D_{ep(i)}}\right]^{n-1}\right\} \qquad (3.59)$$

Reynolds number

$$Re_{p(i)} = \frac{(D_{ep(i)}) * (\rho_{p(i)}) * (v_{p(i)})}{\mu_{ap(i)}} \qquad (3.60)$$

Hydrostatic pressure

$$P_{hp(i)} = \rho_{p(i)} \times g \times (x_i - x_{i-1}) + P_{hp(i-1)} \qquad (3.61)$$

$P_{hp(0)}$ is known we set it for exemple equal to 0 Pa

Friction factor

$$a = \frac{\log_{10}(n) + 3.93}{50} \qquad (3.62)$$

$$b = \frac{1.75 - \log_{10}(n)}{7} \qquad (3.63)$$

$$f_{p(i)} = \frac{16}{Re_{p(i)}} \text{ for } Re_{p(i)} < Re_{lam} \qquad (3.64)$$

$$f_{p(i)} = \left(\frac{16}{Re_{lam}}\right) + \left(\frac{Re_{p(i)} - Re_{lam}}{800}\right) \times \left(\left(\frac{a}{Re_{tur}^{b}}\right) - \left(\frac{16}{Re_{lam}}\right)\right) \text{ for } Re_{lam} \leq Re_{p(i)} \leq Re_{tur} \qquad (3.65)$$

$$f_{p(i)} = \frac{a}{Re_{p(i)}^{b}} \text{ for } Re_{p(i)} > Re_{tur} \qquad (3.66)$$

Pressure loss

$$\Delta P_{p(i)} = \left(\frac{f_{a(i)}\left(\rho_{a(i)}\right)\left(v_{a(i)}\right)^2}{2D_{ha(i)}}\right)(x_i - x_{i-1}) \qquad (3.67)$$

Cumulative pressure loss

$$PL_{cum,p(0)} = \Delta P_{p(i)} \qquad (3.68)$$

$$PL_{cum,p(i)} = PL_{cum,p(i-1)} + \Delta P_{p(i)} \qquad (3.69)$$

Dynamic pressure

$$P_{dp(i)} = P_{hp(i)} + PL_{cum,p(i)} \qquad (3.70)$$

Conclusion

The differential equations governing the heat transfer in the wellbore are established by an energy balance between the formation and the wellbore and by some mathematical developments such as the TAYLOR's development. To improve the model we proposed three different inlet mud temperature models. The equations for the pressure calculation are also given in this chapter.

Chapter 04: Presentation of "WELL-TEMP" code.

Introduction

We concluded from the last chapter that an analytical solution for the temperature distribution is not available. A numerical algorithm is imposed. In this chapter the algorithm for the numerical solution is developed, and a computer code "WELL-TEMP" under MATLAB environment is implemented. The steps from the inputs to the outputs which constitutes this code are explained in details. The results of the present model compare well with the analytical results. This validates the "WELL-TEMP" code.

4.1. Numerical approach

In this section, a numerical approach for the temperature distribution is presented. The wellbore is discretisized into small finite element. For each element of the wellbore, all the parameters that vary throughout the wellbore are updated and treated as constants over the individual element length. This allows equation (3.19) to be solved by the Undetermined Coefficients method. Since a numerical approach is implemented, the notation of the discretisized wellbore given in figure 4.1 is now employed. The index i refers to the element in the discretisized wellbore.

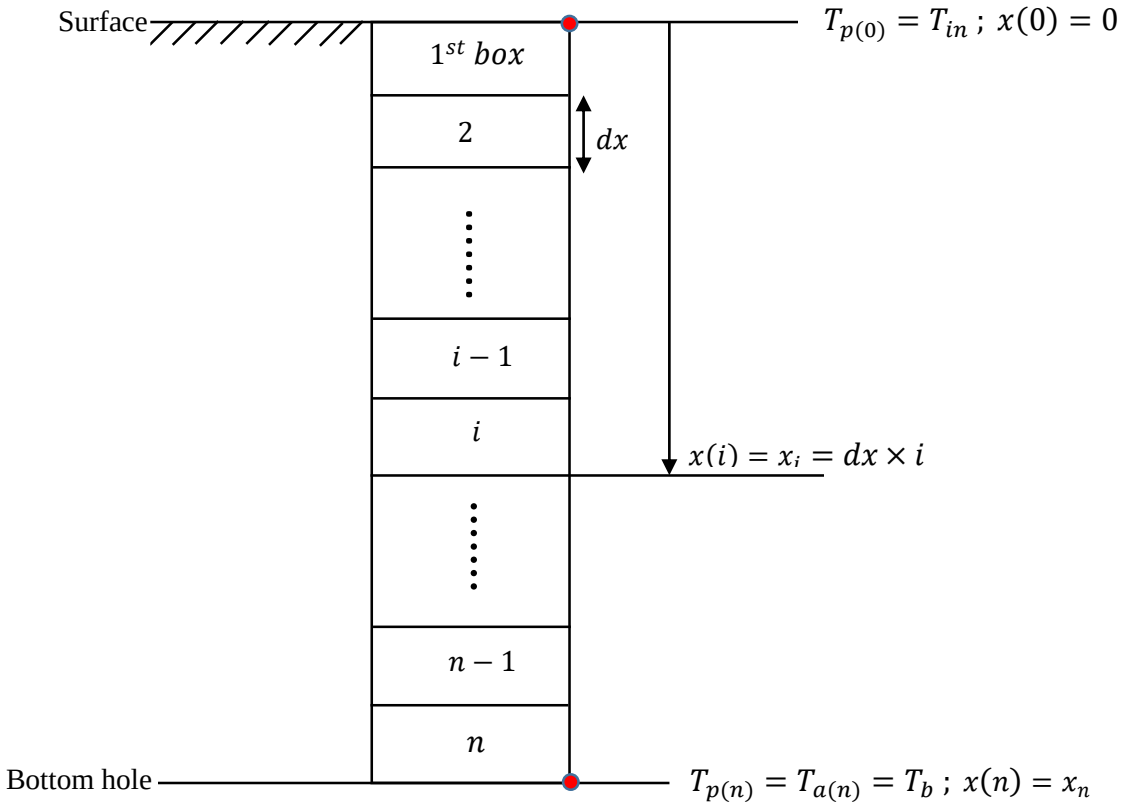

Fig 4.1 discretized wellbore

The formation temperature T_f in equation (3.21) varies with depth. For a vertical wellbore, it is common to express the formation temperature with a constant surface temperature and a linear geothermal gradient such as in equation (4.1).

$$T_f(x) = T_s + Gx \qquad (4.1)$$

But the objective of this work is to develop a temperature model for deviated wellbores. Taking advantage of the numerical approach, the following function has been implemented:

$$T_{f(i)} = T_{f(i-1)} + G_{(i)}.\cos\left(I_{(i)}\right).\left(x_{(i)} - x_{(i-1)}\right) \qquad (4.2)$$

Here, $T_{f(i-1)}$ and $x_{(i-1)}$ refers to the formation temperature and the measured depth at box i–1, and $x_{(i)}$, $I_{(i)}$ and $G_{(i)}$ represents measured depth and the angle of inclination and the geothermal gradient the for box i. Equation (3.19) can now be expressed as:

$$\frac{d^2T_{p(i)}}{dx^2} - D_i\frac{dT_{p(i)}}{dx} - A_iB_iT_{p(i)} = -A_iB_i\left[T_{f(i-1)} + G_{(i)}.\cos\left(I_{(i)}\right).\left(x_{(i)} - x_{(i-1)}\right)\right]$$
$$-\frac{B_i + C_i}{m_{p(i)}c_{pp}}\frac{\phi_{p(i)}}{dx_{(i)}} - \frac{A_i}{m_{a(i)}c_{pa}}\frac{\phi_{a(i)}}{dx_{(i)}} \qquad (4.3)$$

Finally, solving the second order inhomogeneous differential equation above yields the general expression for the temperature distribution in the drill pipe:

$$T_{p(i)} = C_{1(i)}e^{\theta_{1(i)}x_i} + C_{2(i)}e^{\theta_{2(i)}x_i} + T_{f(i-1)} + G_i.\cos(I_i)\,x_i - G_i.\cos(I_i)\,x_{i-1} - \frac{D_i}{A_iB_i}G_i.\cos(I_i)$$
$$+\frac{B_i + C_i}{A_iB_i}.\frac{1}{m_{p(i)}c_{pp}}.\frac{\phi_{p(i)}}{dx_i} + \frac{1}{B_im_{a(i)}c_{pa}}.\frac{\phi_{a(i)}}{dx_i} \qquad (4.4)$$

Furthermore, substituting equation (4.4) for T_p in equation (3.18) gives the general solution of the temperature distribution in the annulus.

$$T_{a(i)} = \left(1 + \frac{\theta_{1(i)}}{A_i}\right)C_{1(i)}e^{\theta_{1(i)}x_i} + \left(1 + \frac{\theta_{2(i)}}{A_i}\right)C_{2(i)}e^{\theta_{2(i)}x_i} + T_{f(i-1)} + G_i.\cos(I_i)\,x_i - G_i.\cos(I_i)\,x_{i-1}$$
$$+\left(\frac{1}{A_i} - \frac{D_i}{A_iB_i}\right)G_i.\cos(I_i)$$
$$+\left(\frac{B_i + C_i}{A_iB_i} - \frac{1}{A_i}\right)\frac{1}{m_{p(i)}c_{pp}}\frac{\phi_{p(i)}}{dx_i} + \frac{1}{B_im_{a(i)}c_{pa}}\frac{\phi_{a(i)}}{dx_i} \qquad (4.5)$$

Where

$$\theta_{1(i)} = \frac{D_i + \sqrt{D_i^2 + 4A_iB_i}}{2} \qquad (4.6)$$

$$\theta_{2(i)} = \frac{D_i - \sqrt{D_i^2 + 4A_iB_i}}{2} \qquad (4.7)$$

Equations (4.4) and (4.5) are solved to determine the wellbore temperature distribution for each element in the wellbore. Note that the following coefficients that are not constant must be determined for each element:

$$C_1, C_2, \theta_1, \theta_2, A, B, C, D$$

Also, note that equations (4.2), (4.4), and (4.5) are valid for:

$$x_{i-1} \leq x \leq x_i$$

4.2. Algorithm

This section presents the developed algorithm for the wellbore temperature distribution. The procedure starts at the bottom of the well and relies on a given temperature to calculate the temperature distribution throughout the wellbore. The bottom of the wellbore and the total number of elements is represented by the letter n in figure 4.1. At this point, it is necessary to give an initial guess for the bottom hole temperature as a boundary condition. A reasonable choice of a boundary condition for a drilling operation is:

$$T_{p(n)} = T_{a(n)} = T_b$$

Where T_b represents the guess of wellbore temperature at the bottom of element number n, as indicated by the red mark in figure 4.1. The corresponding depth and angle of inclination are given by:

$$x = dx \times n$$

$$I = I_n$$

Where x is the measured depth and dx is the measured depth of a single element.

Substituting T_p and T_a with T_b in equations (4.4) and (4.5) gives a system of two equations with two variables, explicitly $C_{1(n)}$and $C_{2(n)}$.

$$T_b = C_{1(n)}e^{\theta_{1(n)}x_n} + C_{2(n)}e^{\theta_{2(n)}x_n} + T_{f(n-1)} + G_n.\cos(I_n)\,x_n$$

$$-G_n.\cos(I_{\mathrm{n}})\,x_{n-1}-\frac{D_n}{A_nB_n}G_n.\cos(I_{\mathrm{n}})+\frac{B_n+C_n}{A_nB_n}.\frac{1}{m_{p(n)}c_{pp}}.\frac{\phi_{p(n)}}{dx_n}+\frac{1}{B_nm_{a(n)}c_{pa}}.\frac{\phi_{a(n)}}{dx_n} \quad (4.8)$$

$$T_b=\left(1+\frac{\theta_{1(n)}}{A_n}\right)C_{1(n)}e^{\theta_{1(n)}x_n}+\left(1+\frac{\theta_{2(n)}}{A_n}\right)C_{2(n)}e^{\theta_2(n)x_n}+T_{f(n-1)}+G_n.\cos(I_{\mathrm{n}})\,x_n-G_n.\cos(I_{\mathrm{n}})\,x_{n-1}+\left(\frac{1}{A_n}-\frac{D_n}{A_nB_n}\right)G_n.\cos(I_{\mathrm{n}})+\left(\frac{B_n+C_n}{A_nB_n}-\frac{1}{A_n}\right)\frac{1}{m_{p(n)}c_{pp}}\frac{\phi_{p(n)}}{dx_n}+\frac{1}{B_nm_{a(n)}c_{pa}}\frac{\phi_{a(n)}}{dx_n} \quad (4.9)$$

Equations (4.8) and (4.9) are valid for:

$$dx(n-1)\le x\le dx.n$$

A convenient method to solve equations (4.8) and (4.9) for $C_{1(n)}$ and $C_{2(n)}$ is matrix multiplication. The coefficients $C_{1(n)}$and $C_{2(n)}$can be determined by rearranging equations (4.8) and (4.9) into the following form:

$$\begin{pmatrix}C_{1(n)}\\C_{2(n)}\end{pmatrix}=\begin{pmatrix}a_n & b_n\\c_n & d_n\end{pmatrix}^{-1}\begin{pmatrix}y_{1(n)}\\y_{2(n)}\end{pmatrix}$$

Where

$$a_n=e^{\theta_{1(n)}x_n}$$

$$b_n=e^{\theta_{2(n)}x_n}$$

$$c_n=\left(1+\frac{\theta_{1(n)}}{A_n}\right)e^{\theta_{1(n)}x_n}$$

$$d_n=\left(1+\frac{\theta_{2(n)}}{A_n}\right)e^{\theta_2(n)x_n}$$

$$y_{1(n)}=T_b-\left(T_{f(n-1)}+G_n.\cos(I_{\mathrm{n}})\,dx_n-\frac{D_n}{A_nB_n}G_n.\cos(I_{\mathrm{n}})+\frac{B_n+C_n}{A_nB_n}\frac{1}{m_{p(n)}c_{pp}}\frac{\phi_{p(n)}}{dx_n}+\frac{1}{B_nm_{a(n)}c_{pa}}\frac{\phi_{a(n)}}{dx_n}\right)$$

$$y_{2(n)} = T_b - \left(T_{f(n-1)} + G_n.\cos(I_n)\, dx_n + \left(\frac{1}{A_n} - \frac{D_n}{A_n B_n}\right) G_n.\cos(I_n) + \left(\frac{B_n + C_n}{A_n B_n} - \frac{1}{A_n}\right) \frac{1}{m_{p(n)} c_{pp}} \frac{\phi_{p(n)}}{dx_n} + \frac{1}{B_n m_{a(n)} c_{pa}} \frac{\phi_{a(n)}}{dx_n} \right)$$

Assuming the coefficients $C_{1(n)}$ and $C_{2(n)}$ are constant for element n, $T_{p(n-1)}$ and $T_{a(n-1)}$ are calculated at the boundary between element n and $n-1$ by using $C_{1(n)}$and $C_{2(n)}$ in equations (2.25) and (2.26) respectively. Note that the depth and angle of inclination at this point are given by:

$$x = dx(n-1)$$

$$I = I_n$$

After $T_{p(n-1)}$ and $T_{a(n-1)}$ have been determined, they will serve as the boundary temperatures for element number $n-1$, and $C_{1(n-1)}$ and $C_{2(n-1)}$ are calculated with the same approach as above to obtain $T_{p(n-2)}$ and $T_{a(n-2)}$. This procedure is repeated for the remaining elements to get the total wellbore temperature distribution. In a general notation, $C_{1(i)}$and $C_{2(i)}$ are calculated based on the boundary temperatures $T_{p(i)}$ and $T_{a(i)}$and used in equations (4.4) and (4.5) to obtain $T_{p(i-1)}$ and $T_{a(i-1)}$. The depth and angle of inclination for element number i becomes:

$$x = dx(i-1)$$

$$I = I_i$$

When i=1 and element number 1 is reached, the depth and the angle of inclination will be

$$x = 0$$

$$I = I_1$$

And equations (4.4) and (4.5) reduce to

$$T_{p(0)} = C_{1(1)} + C_{2(1)} + T_{f(0)} - \frac{D_1}{A_1 B_1} G_1.\cos(I_1) + \frac{B_1 + C_1}{A_1 B_1}.\frac{1}{m_{p(1)} c_{pp}}.\frac{\phi_{p(1)}}{dx_1} + \frac{1}{B_1 m_{a(1)} c_{pa}}.\frac{\phi_{a(1)}}{dx_1} \qquad (4.10)$$

$$T_{a(0)} = \left(1 + \frac{\theta_{1(1)}}{A_1}\right) C_{1(1)} + \left(1 + \frac{\theta_{2(1)}}{A_1}\right) C_{2(1)} + T_{f(0)} + \left(\frac{1}{A_1} - \frac{D_1}{A_1 B_1}\right) G_1.\cos(I_1) + \left(\frac{B_1 + C_1}{A_1 B_1} - \frac{1}{A_1}\right) \frac{1}{m_{p(1)} c_{pp}} \frac{\phi_{p(1)}}{dx_1} + \frac{1}{B_1 m_{a(1)} c_{pa}} \frac{\phi_{a(1)}}{dx_1} \qquad (4.11)$$

With this last step, the temperature distribution for the entire wellbore has been calculated. To summarize, consider the following stepwise approach as a representation of the algorithm for calculating the wellbore temperature distribution:

- Give a guess for the bottom hole temperature T_b.
- Determine the coefficients $C_{1(n)}$ and $C_{2(n)}$.
- Calculate $T_{p(n-1)}$ and $T_{a(n-1)}$.
- Set $i = n - 1$ and update the coefficients that are not constant.
- Determine $C_{1(i)}$ and $C_{2(i)}$.
- Calculate $T_{p(i-1)}$ and $T_{a(i-1)}$.
- Set $i = i - 1$ and repeat step 4 to 6.
- Stop when $i = 1$.

4.3. Shooting method

The algorithm presented in section 4.2 may be defined as a boundary value problem with the following set of equations and boundary conditions:

$$T_{p(i)} = C_{1(i)} e^{\theta_{1(i)} x_i} + C_{2(i)} e^{\theta_{2(i)} x_i} + T_{f(i-1)} + G_i . \cos(I_i)\, x_i - G_i . \cos(I_i)\, x_{i-1} - \frac{D_i}{A_i B_i} G_i . \cos(I_i) + \frac{B_i + C_i}{A_i B_i} . \frac{1}{m_{p(i)} c_{pp}} . \frac{\phi_{p(i)}}{dx_i} + \frac{1}{B_i m_{a(i)} c_{pa}} . \frac{\phi_{a(i)}}{dx_i}$$

$$T_{a(i)} = \left(1 + \frac{\theta_{1(i)}}{A_i}\right) C_{1(i)} e^{\theta_{1(i)} x_i} + \left(1 + \frac{\theta_{2(i)}}{A_i}\right) C_{2(i)} e^{\theta_{2(i)} x_i} + T_{f(i-1)} + G_i . \cos(I_i)\, x_i - G_i . \cos(I_i)\, x_{i-1} + \left(\frac{1}{A_i} - \frac{D_i}{A_i B_i}\right) G_i . \cos(I_i) + \left(\frac{B_i + C_i}{A_i B_i} - \frac{1}{A_i}\right) \frac{1}{m_{p(i)} c_{pp}} \frac{\phi_{p(i)}}{dx_i} + \frac{1}{B_i m_{a(i)} c_{pa}} \frac{\phi_{a(i)}}{dx_i}$$

$$T_{p(n)} = T_{a(n)} = T_b$$

$$T_{p(0)} = T_{in}$$

Where T_{in} is the drill pipe inlet temperature.

A guess is made for T_b to calculate the total wellbore temperature distribution. If the guess of T_b results in a temperature distribution where $T_{p(0)}$ satisfies the boundary condition at x=0, the problem is solved. If the boundary condition is not satisfied, T_b is adjusted until the solution converges.

This approach takes advantage of the Intermediate Value Theorem which states that if $f(x)$ is a continuous function for a given interval $[a, b]$ and $f(a)$ and $f(b)$ have opposite sings, there must be a point c on the interval $[a, b]$ that gives $f(c) = 0$. An illustration of this statement is presented in figure 4.2. The Bisection method is used to find the root of $f(x)$ by repeatedly bisecting the interval $[a, b]$ until there is a midpoint c in the interval such that $f(c)$ converges to 0.

Normally; a tolerance is set such that a solution is accepted when

$$|f(c)| < tolerance$$

To apply the Bisection Method to the current calculation procedure, the initial interval $[a, b]$ is defined as $[0\ , 2 \times T_{f(n)}]$ to ensure that the convergence is reached rapidly, and f is defined as.

$$f(T_b) = T_{p(0)} - T_{in}$$

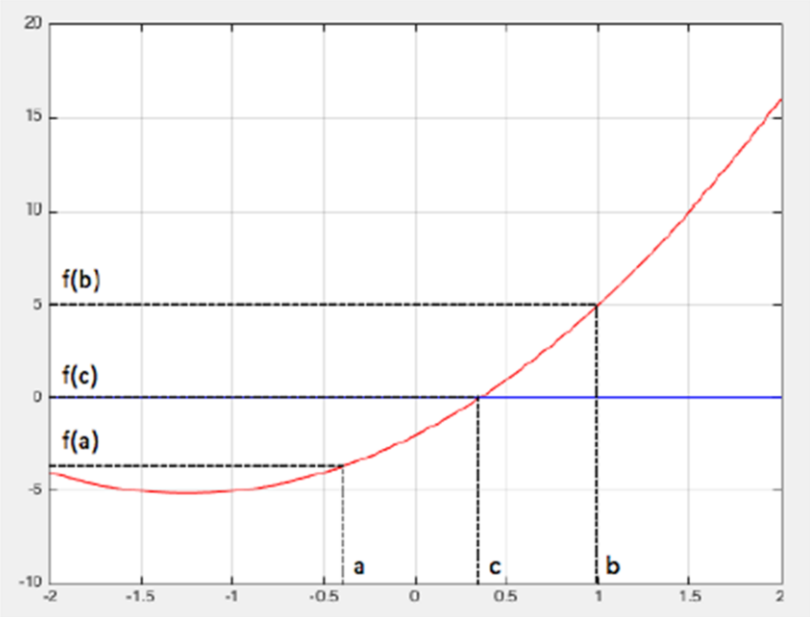

Fig 4.2 Intermediate Value Theorem

4.4. "WELL – TEMP" architecture

Inputs

- In this part of the MATLAB program the user enters the geometry (radius, depth) of the wellbore.
- All the thermo- physical properties of the drill pipe, casings, cements and formations are specified.
- The user choses the inlet mud temperature model according to the previous section.
- The user choses if he enters the effect of pressure and temperature on density and viscosity or not, same for energy sources therefore the model offers three options for the temperature calculation.

    1. Without effect of pressure and temperature on density and viscosity and without the effect of energy sources. If the user just wants an estimation of the temperature, and the execution time is very short for this option.
    2. With effect of pressure and temperature on density and viscosity and without the effect of energy sources. If the user wants more precision, and the execution time is longer than the first option.
    3. With the effect of pressure and temperature on density and viscosity and with the effect of energy sources. If the user wants maximum precision, and the execution time is greater than that of the second option.

Figure 4.3 shows some examples of the inputs of our model

```
%          od_oh,   od_c,   id_c,   top_md, bottom_md, ff,   K_csg, C_csg, d_csg,  TOC,  K_cement, C_cement,  d_cement,  Type
wellbore_data=[26     18+5/8  17.5      0    1000       0.3    48     500    1      0     0.99       838       2         0 ;
               16     13+3/8  12.3      0    2000       0.3    48     500    1      0     0.99       838       2         0 ;
               12.25  9+5/8   8.7       0    4000       0.3    48     500    1      0     0.99       838       2         0 ;
               8+3/8  8+3/8   8+3/8     0    4572       0.3    00     000    1      0     0          0         0         1 ];

        %    top_md, bottom_md,  K_for,   C_for,  d_for,   geothermal gradient (C°/m)
formation_data=[0       4572       1.75     838    2.64      0.02315];

Include_temperature_pressure_effect_on_mud=0;
Include_pressure_loss_energy_source_on_mud=0;
Include_joule_thomson_effect_energy_source_on_mud=0;
constant_inlet_temperature=1;
changing_inlet_temperature=0;
canstant_differance_temperture=0;
```

Fig 4.3 some inputs of the model

Output

- The program first calculates the distribution of temperature without entering the effect of pressure and temperature on viscosity and density and without taking in consideration energy source terms.
- Then the program recalculates the temperature's distribution using density and viscosity models and also energy source terms.

The steps that are followed in the model are explained below:

Step 1: inputs.

Step 2: calculation of temperature and of pressure at constant density and viscosity and without energy source terms.

Step 3: using the temperature and the pressure calculated in step 2 to generate the new density and viscosity for each element.

Step 4: recalculate the temperature and the pressure using density and viscosity calculated in step 3 and taking into account this time energy source terms

Step 5: calculate the difference between the temperatures of step 2 and step 4.

Step 6.1: if the difference < tolerance; stop.

Step 6.2: if the difference > tolerance; calculate the new density and viscosity using the temperature and the pressure calculated in step 4.

Step 7: repeat steps from 4 to 6.2 until convergence.

4.5. Model Validation

To validate the efficiency of the developed «WELL-TEMP" code, we adopted the data set used by Holmes and Swift (1970) as shown in Table 4.1 Applications of both the Holmes and Swift (1970) model and Kabir et al. (1996) model form the foundation for verification of the possible applications of the present model of this study. Fig. 4.4 and Fig 4.5 compares the temperature profiles of the conduit and the annular temperature for the present model with Kabir et al. (1996) and that of the Holmes and Swift (1970).

Table 4. 1 well and mud circulating properties

Well geometry	
Well depth, m	4572
Drill stem OD, m	0,1524
Drill-bit size, m	0,2032
Circulating rate, l/min	795
Inclinations, deg	0
Mud properties	
Inlet temperature, °C	23.889
Thermal conductivity, W/(m°C)	1.73
Specific heat, J/(kg.K)	1676
Density, kg/m^3	1198.264
Formation properties	
Thermal conductivity, W/(m°C)	2.25
Specific heat, J/(kg.K)	838
Density, kg/m^3	2640
Surface earth temperature, °C	15.278
Geothermal gradient, °C/m	0.02315

The difference in temperature profiles due to incorporating the transient conduction of thermal energy within the formation represented by 44 hours to calculate the T_D.

Figure 4.4 shows the temperature distributions for the three models: Holmes and Swift (1970) and for Kabir et al. (1996) and for the "WELL-TEMP". It is observed from figure 4.4 that the temperature at the top compares well, however at the bottom hole a difference in the temperature of 10°C between the present model and the Holmes and Swift (1970). This is understandable because different approaches result in different temperature distributions due to inherent different assumptions. But it is important to notice that

the trend is essentially the same. We think that an adjustment in the transfer heat coefficients is required to enhance the model. This will be done in the following.

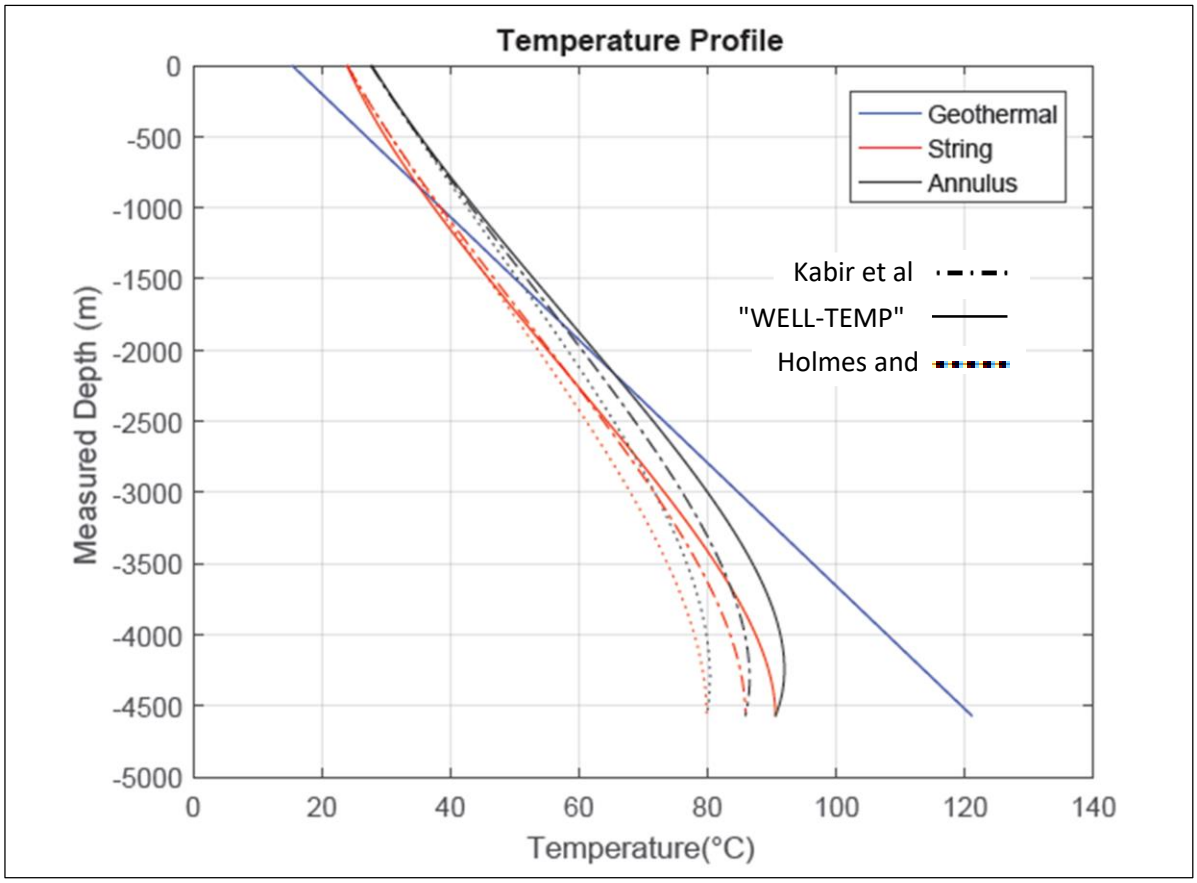

Fig 4.4 Comparison of steady state temperature distribution of 3 methods with the same heat transfer coefficients as Holmes; Ua=5.67 Up=200.1 W/m^{2}K

As suggested above, heat transfer coefficients adjustment (U_a , U_p) have been included in the "WELL - TEMP" model. Figure 4.5 represents the temperature distributions of the three models: Holmes and Swift (1970) and for Kabir et al. (1996) and for the "WELL-TEMP". It is now observed that when the adjustment has been made that the temperature at a depth of 4500m (bottom hole) coincides with the analytical approach. In fact, the bottom hole temperatures agrees within a margin of 1.5°C.

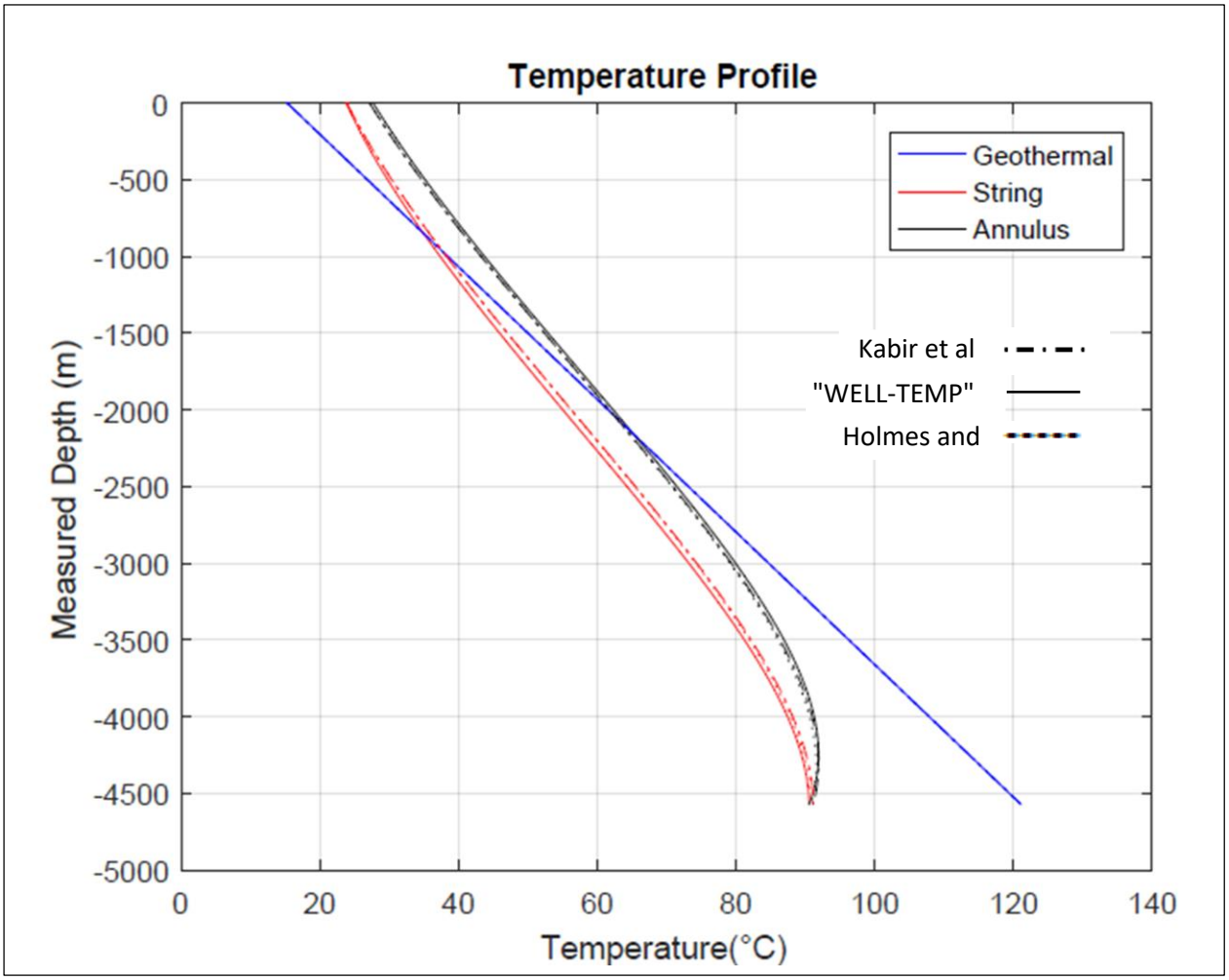

Fig 4.5 Comparison of steady state temperature distribution of 3 methods with adjusted heat transfer coefficients

Conclusion

In this chapter the numerical solution is presented along with its algorithm to calculate the temperature distribution. Then the "WELL-TEMP" code is detailed from the inputs to the outputs. A validation of the "WELL-TEMP" code is achieved based on existing analytical models (KABIR and HOLMES).

Since the model is well validated we can now go to the sensitivity analysis presented in the next chapter.

Chapter 05: Results and discussions

Introduction

In this section, a sensitivity analysis of the developed temperature model is presented with respect to drilling operations. The objective is to determine to what extent a set of parameters of the temperature model will impact the temperature distribution. For the analysis of a given parameter, all the other parameters of the base case (Table 4.1) remain constant. We will start by investigation the flow rate, then other parameters are investigates such as drilling fluid properties.

5.1. Flow rate

To investigate the effect of the flow rate on the temperature distribution, simulations have been performed by varying the flow rate from 100 l/min to 3000 l/min. The results of a flow rates of 500 l/min and 2000 l/min are given by figures 3.1 and 3.2 respectively.

Inspecting the results reveals that the flow rate imposes a significant effect. Increasing the flow rate results in a decrease of bottom hole temperature.

Another effect is that with increasing the flow rate, the temperature distributions in the drill pipe and in the annulus approach each other. For a flow rate of 500 l/min, the temperature difference between the drill pipe inlet and the annulus outlet is approximately 17 °C. The simulation results with a flow rate of 2000 l/min give a temperature difference of only 10 °C.

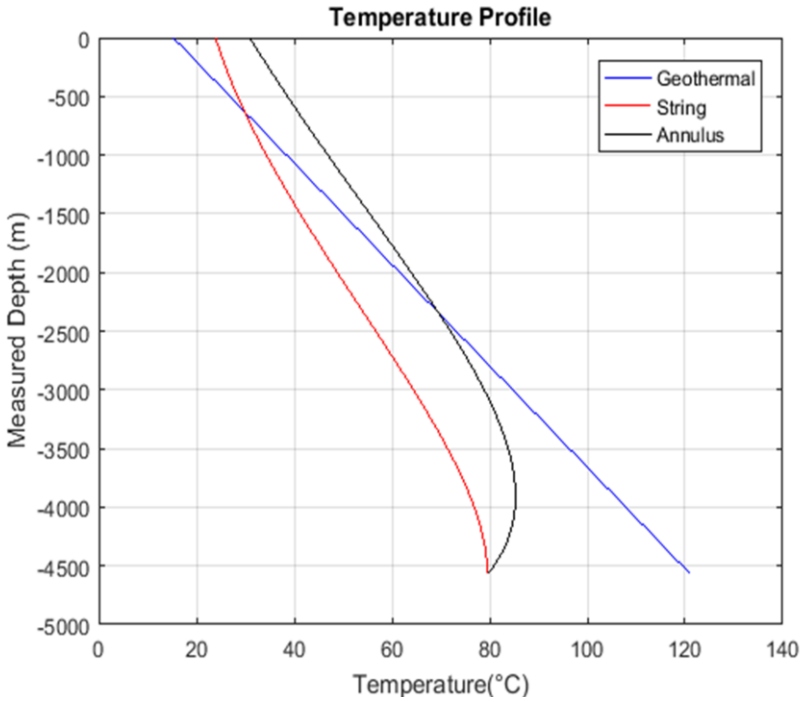

Fig 5. 1 Temperature distribution - flow rate: 500 l/min

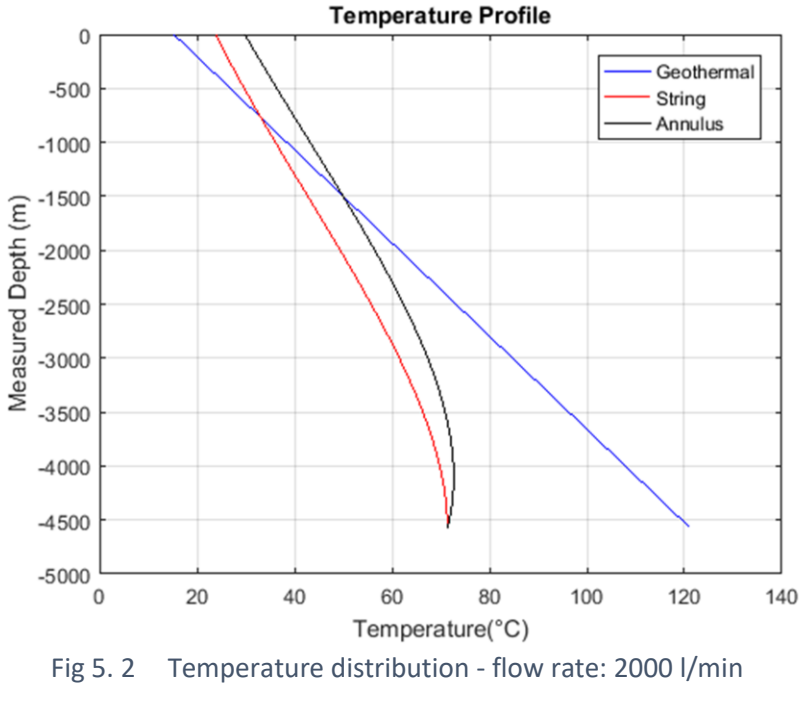

Fig 5. 2 Temperature distribution - flow rate: 2000 l/min

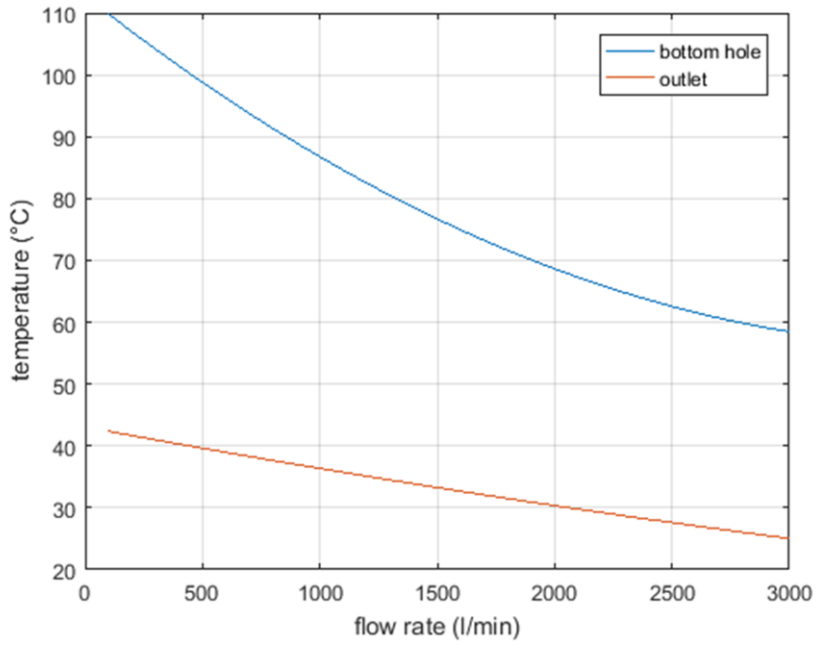

Fig 5. 3 Temperature vs. flow rate

5.2. Specific heat capacity

Specific heat capacity is defined as the amount of heat per unit mass required to increase the temperature of an object by one Kelvin. To determine how sensitive the wellbore temperature distribution is to drilling fluid specific heat capacity, simulations are performed with values in the range of 500-3000 J/kg-°C.

Figures 5.4 and 5.5 show the results for specific heat capacities of 1000 and 2000 J/kg-°C respectively. Comparing these results, it is evident that decreasing the specific heat capacity will increase the temperatures in the wellbore. The maximum temperatures for the 1000 J/kg-°C case have increased with 40% in the pipe and 31% in the annulus compared to the 2000 J/kg-°C case, indicating that the specific heat capacity has a significant effect on the temperature distribution.

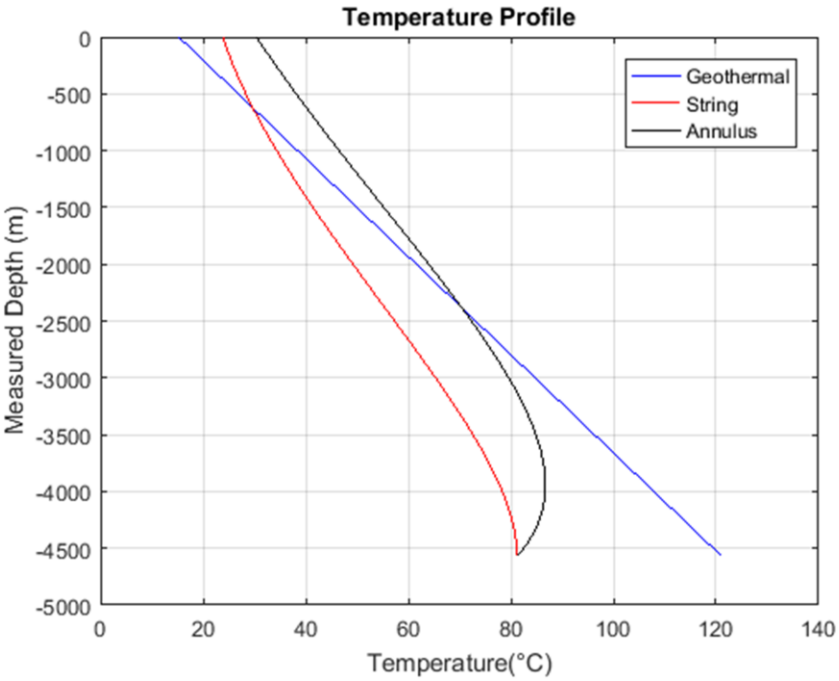

Fig 5. 4 Temperature distribution - specific heat capacity: 1000 J/kg-°C

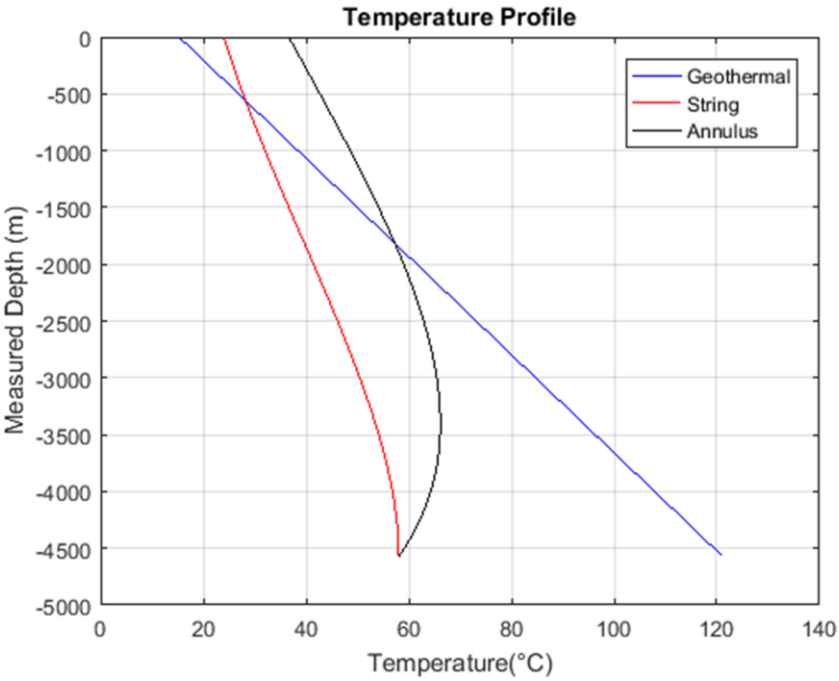

Fig 5.5 Temperature distribution - specific heat capacity: 2000 J/kg-°C

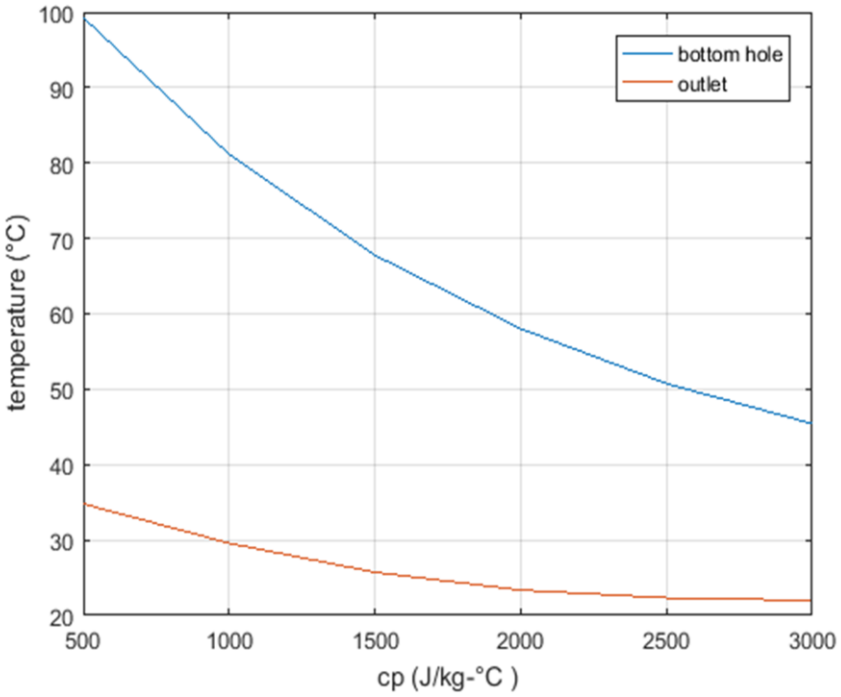

Fig 5. 6 Temperature vs. specific heat capacity

5.3. Thermal conductivity

Drilling fluid

A range of thermal conductivity from 0.5 to 3 W/m-°C have been considered in the simulations. The results for thermal conductivities of 1 and 2 W/m-°C are presented in figures 3.7 and 3.8 respectively. For the first case, a decrease of temperatures is found compared to the base case (k_{fluid} =1.73 W/m-°C). An increase of temperatures is found in the results with a conductivity of 2 W/m-°C. For example, the difference between the maximum temperature of the base case and the case with 1 W/m-°C is about 9%. This indicates that the drilling fluid thermal conductivity makes a difference, but not as pronounced as the flow rate effects. The results for the entire range of considered thermal conductivity values are presented in figure 5.9.

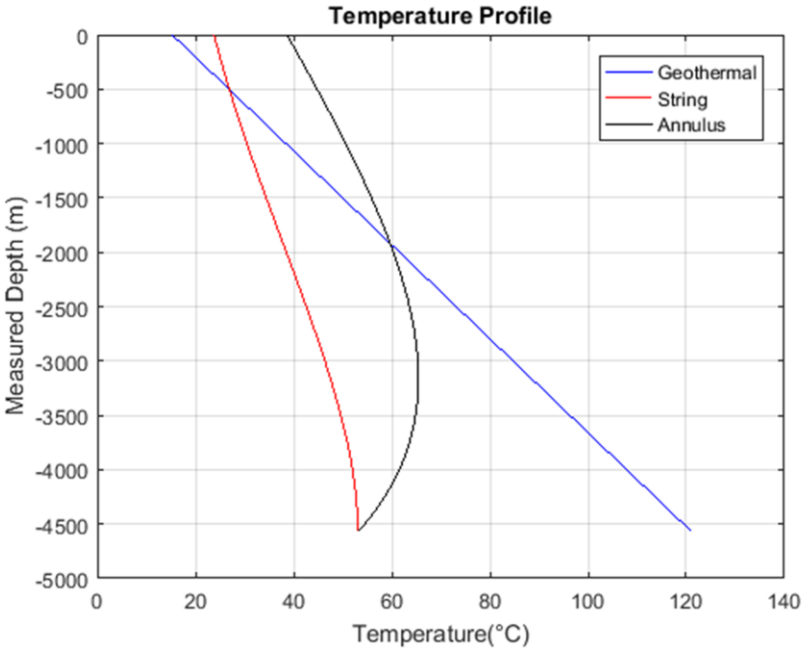

Fig 5. 7 Temperature distribution - thermal conductivity: 1 W/m-°C

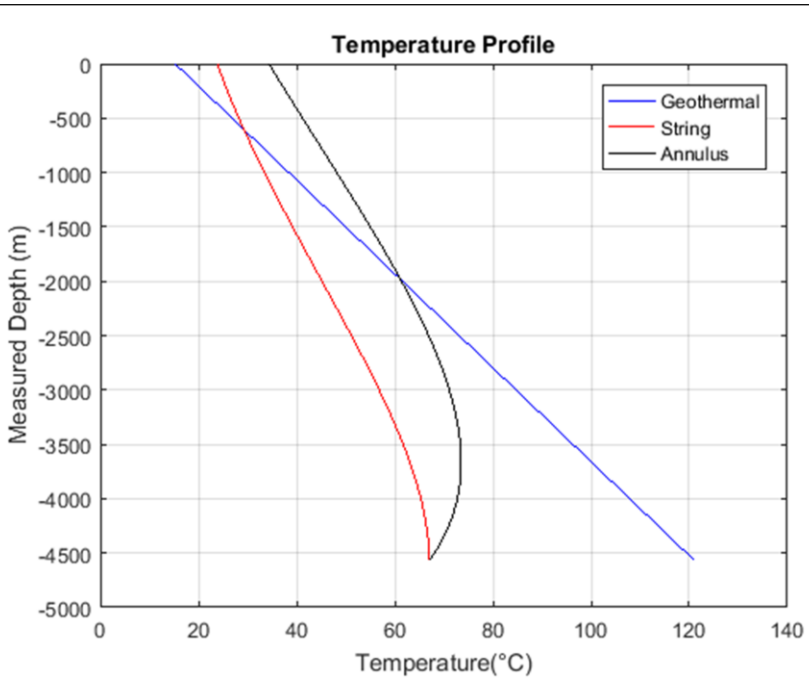

Fig 5. 8 Temperature distribution - thermal conductivity: 2 W/m-°C

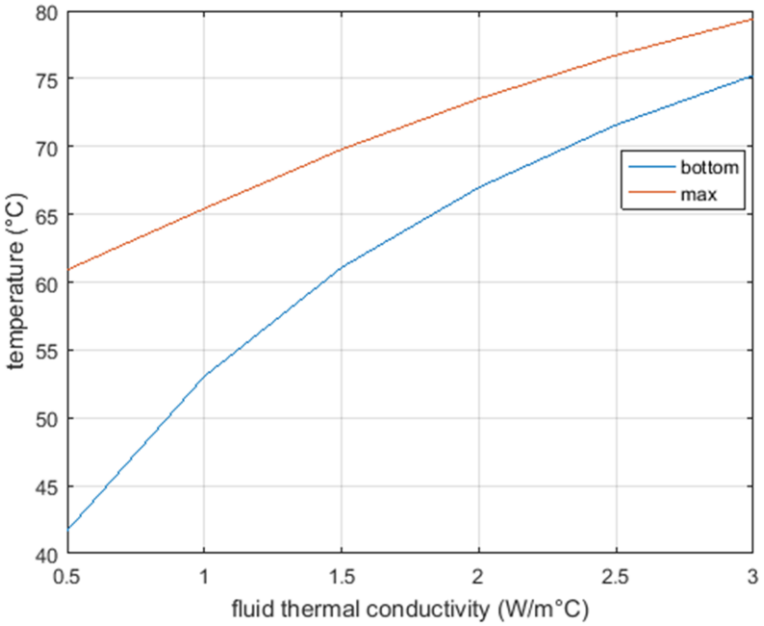

Fig 3. 9 Temperature vs. drilling fluid thermal conductivity

Formation

The thermal conductivity of the formation will affect the heat transfer process at the annulus/formation interface. The simulation results include thermal conductivities in the range of 1.5 to 3.5 W/m-°C.

Figure 5.10 represents the temperature distribution of the fluid with a formation conductivity of 1.75 W/m-°C. Compared to the case where the formation conductivity is 3 W/m-°C represented in figure 5.11; the bottom hole temperature has been increased by 5°C.

Increasing the thermal conductivity will result in increasing the temperature distribution, but it will not produce a large effect as seen with the flow rate and the specific heat capacity.

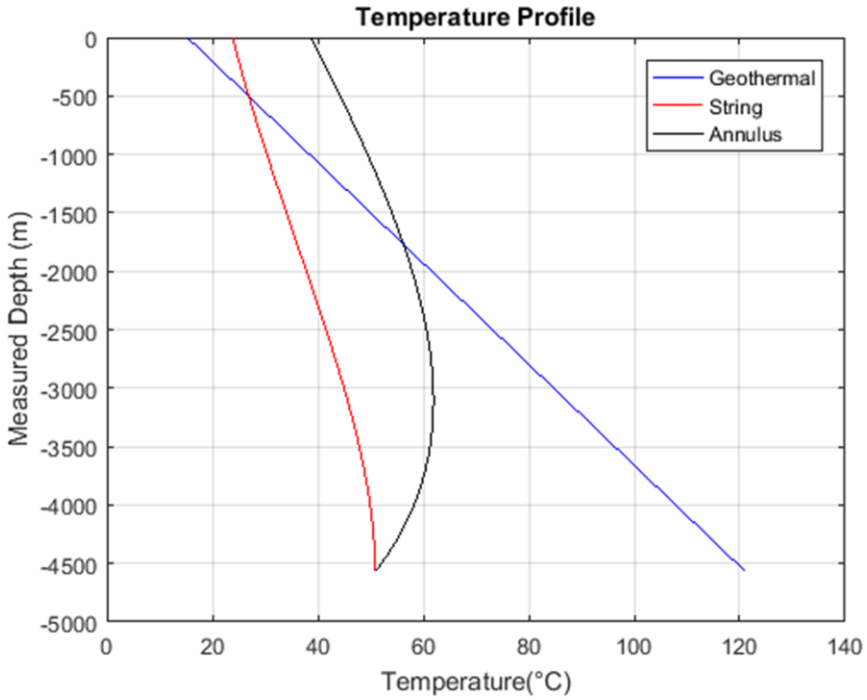

Fig 5. 10 Temperature distribution – formation thermal conductivity: 1.75 W/m-°C

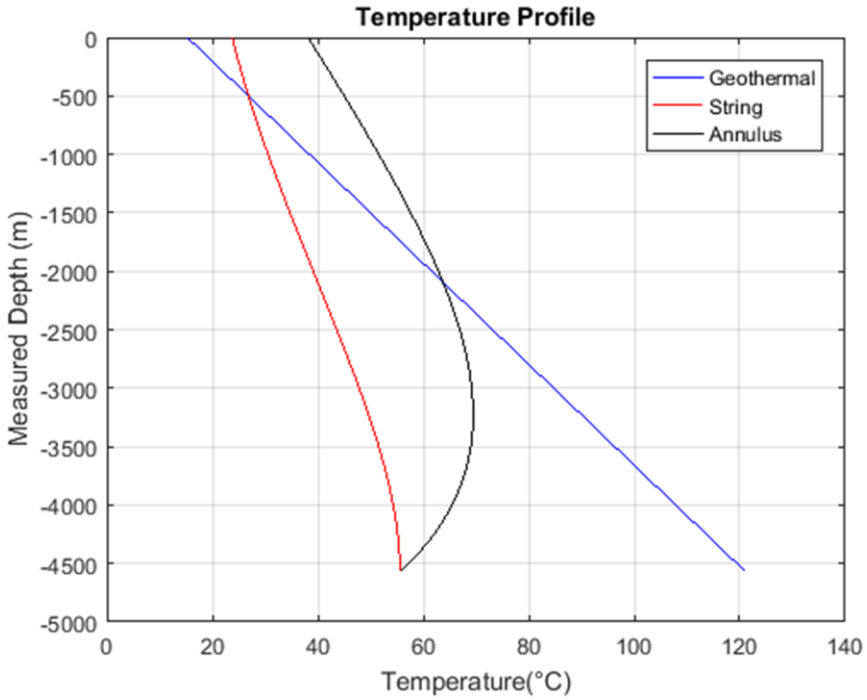

Fig 5. 11 Temperature distribution – formation thermal conductivity: 3 W/m-°C

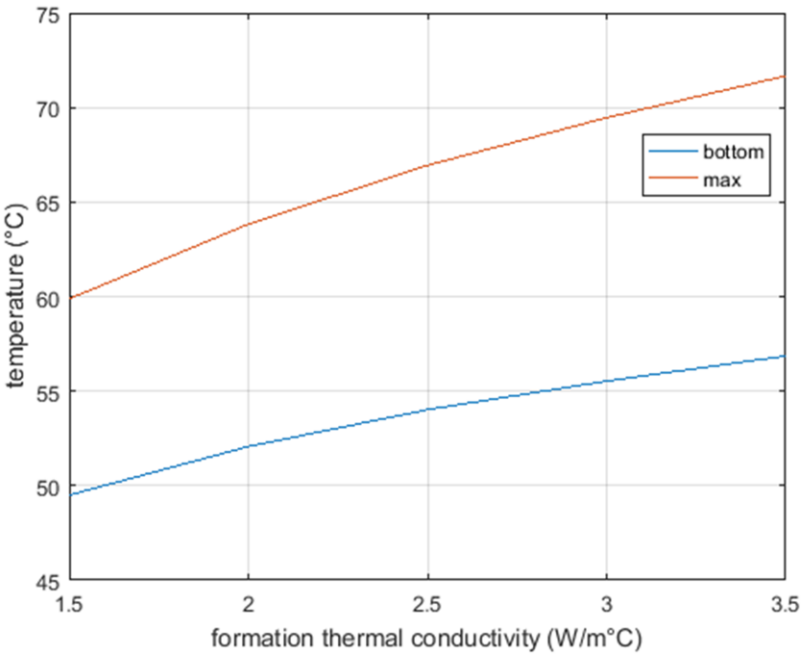

Fig 5. 12 Temperature vs. formation thermal conductivity

Drill pipe

The drill pipe thermal conductivity impacts the rate of conductive heat transfer across the drill pipe wall. Simulations are performed over a range of 10 to 100 W/m-°C.

Figures 5.13 - 5.14 give the simulation results for the pipe thermal conductivity of 30 and 80 W/m-°C respectively. From figure 5.15 which represents the changes in temperature by varying the thermal conductivity of the pipe we conclude that the effect is minimal and it can be neglected.

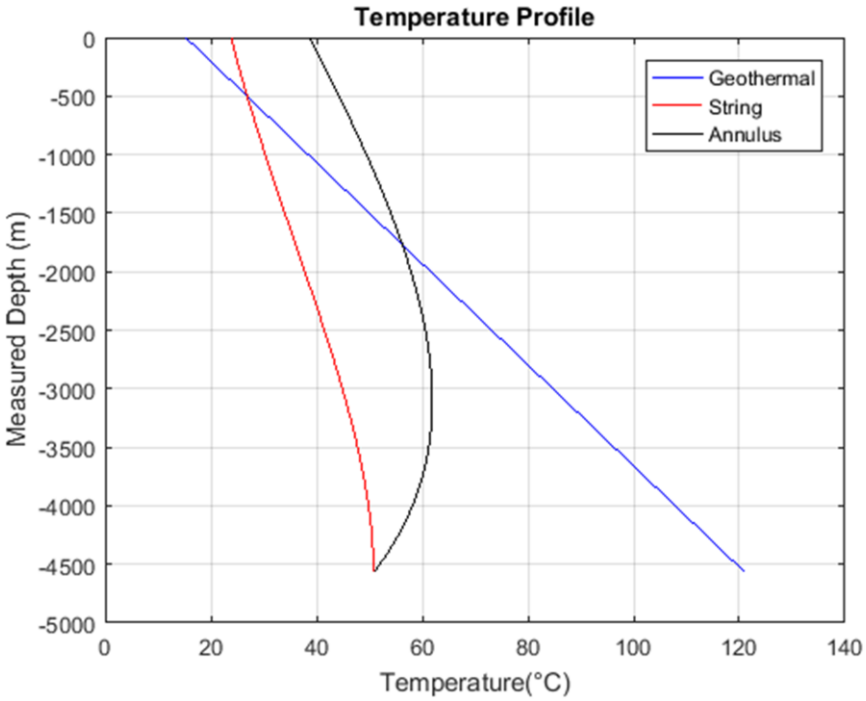

Fig 5. 13 Temperature distribution – drill pipe thermal conductivity: 30 W/m-°C

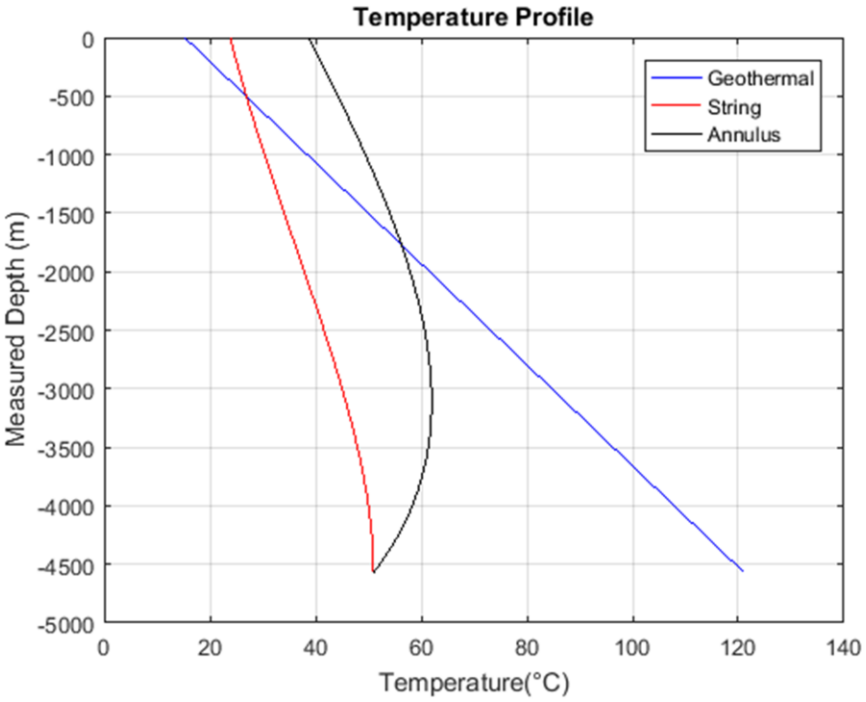

Fig 5.14 Temperature distribution – drill pipe thermal conductivity: 80 W/m-°C

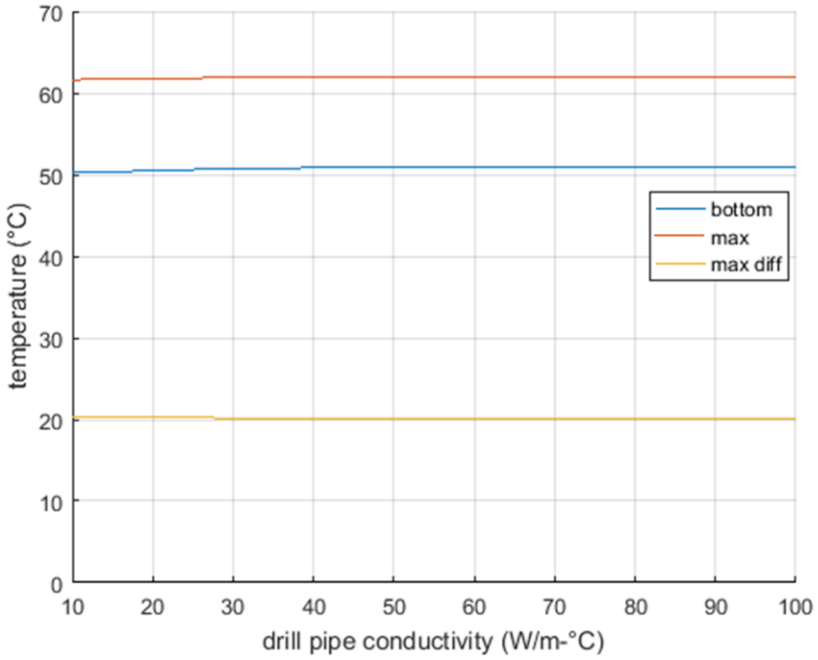

Fig 5. 15 Temperature vs. drill pipe thermal conductivity

5.5. Drilling fluid density

The density model employed in this thesis is based on an OBM with a reference point of 1198.3 kg/m^3 at ambient conditions. The fluid behavior with respect to pressure and temperature has been established through a PVT analysis. To determine the effect of drilling fluid density on the temperature distribution, the reference point is varied over a range of 1000-2000 kg/m^3. Figures 5.16 and 5.17 give the results for drilling fluids with a density of 1000 and 2000 kg/m^3 respectively. Increasing the density results in an overall reduction of wellbore temperature. Comparing the maximum temperature of the 1000 kg/m^3 case with the results of 2000 kg/m^3 gives a reduction of 33%. The effect is much like the one experienced with flow rate.

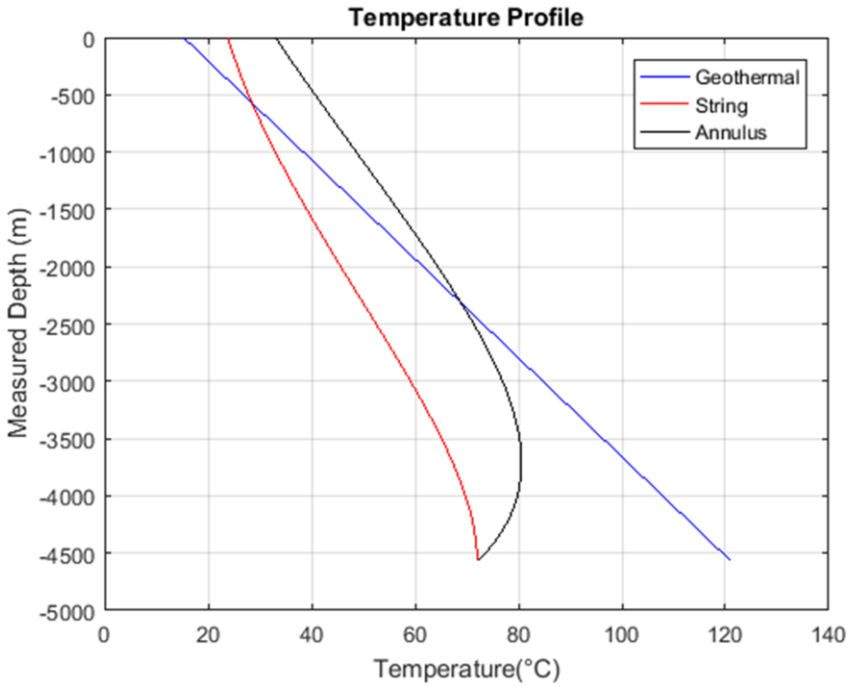

Fig 5. 16 Temperature distribution – density: 1000 kg/m^3

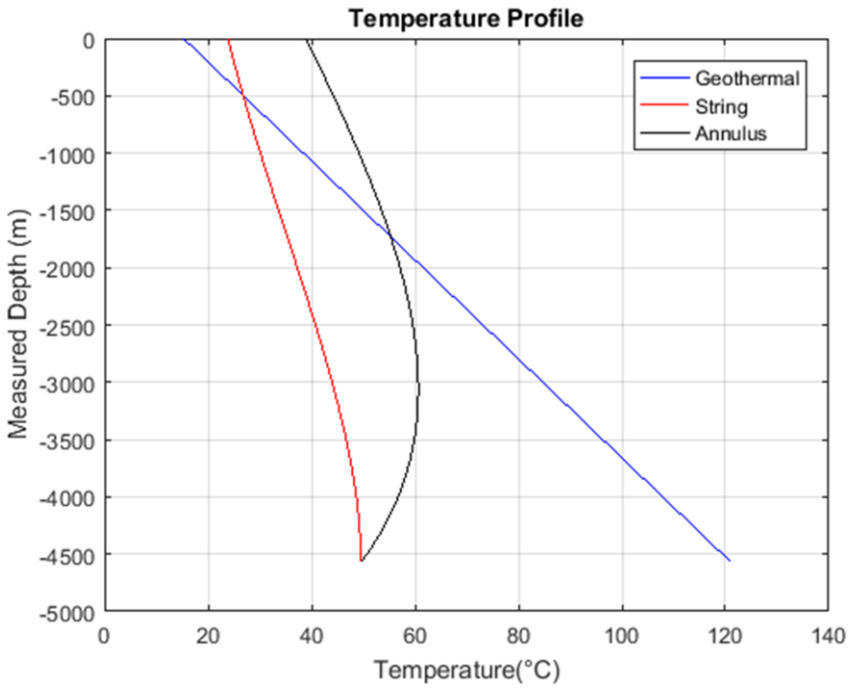

Fig 5. 17 Temperature distribution – density: 1700 kg/m^3

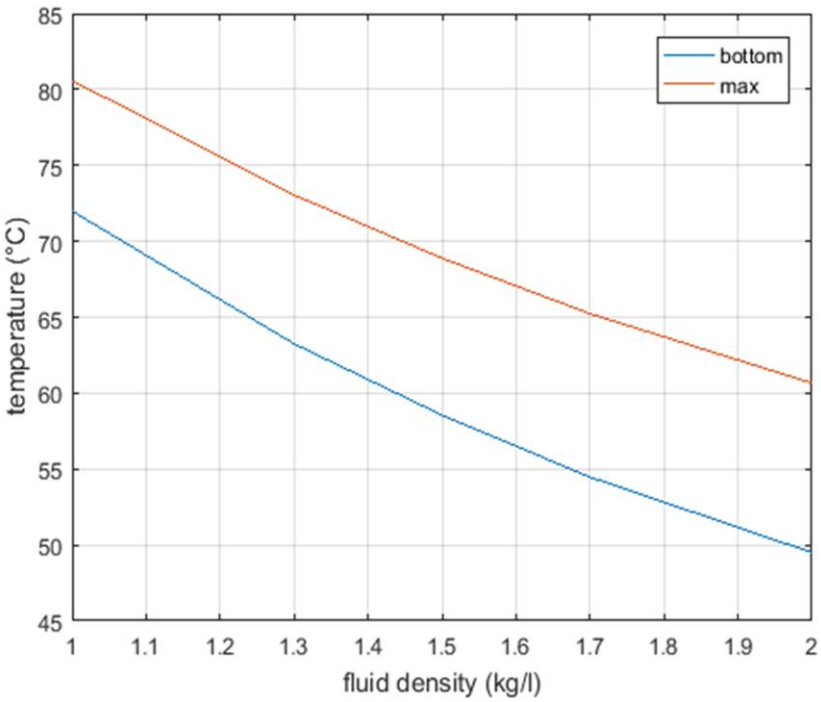

Fig 5. 18 Temperature vs. drilling fluid density

5.6. Geothermal gradient

The geothermal gradient represents the rate of increase in formation temperature with depth, Simulations are performed for geothermal gradients in the range of 10-40 °C/km.

Figures 5.19 and 5.20 represent the temperature distributions with a geothermal gradient of 13.15 and 33.15 °C/km.

Inspecting figures 5.19 and 5.20 reveals that the overall temperature distribution increases with increasing the geothermal gradient. Also, note how the maximum formation temperature increases from about 70 °C in figure 3.19 to over 110 °C in figure 5.20. Figure 5.21 represents a summary of the results, and the temperature increases with the geothermal gradient.

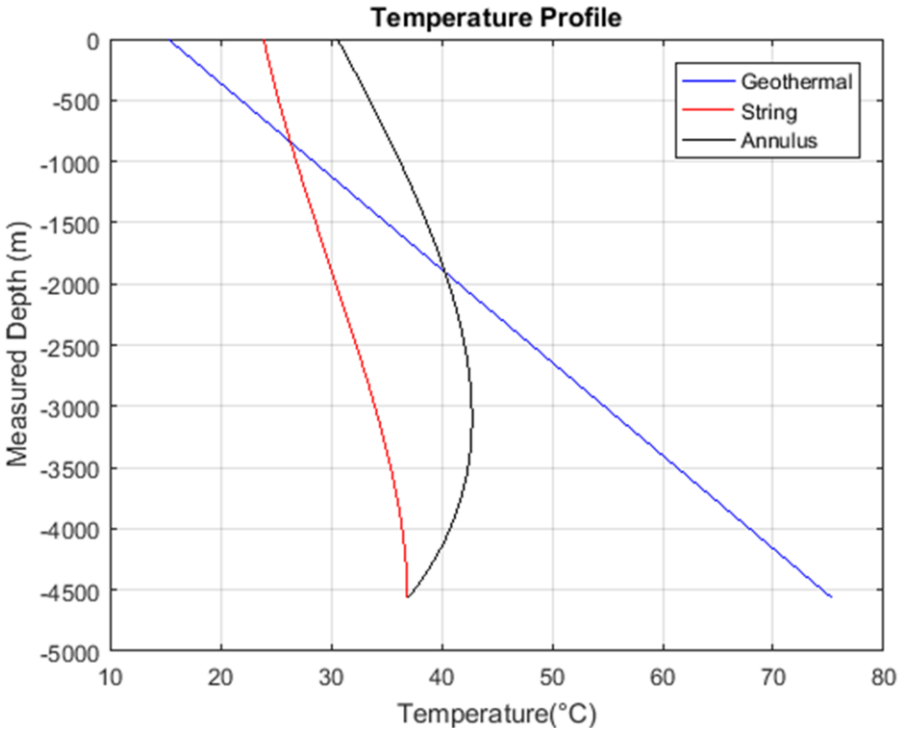

Fig 5. 19 Temperature distribution – geothermal gradient: 13.15 °C/km

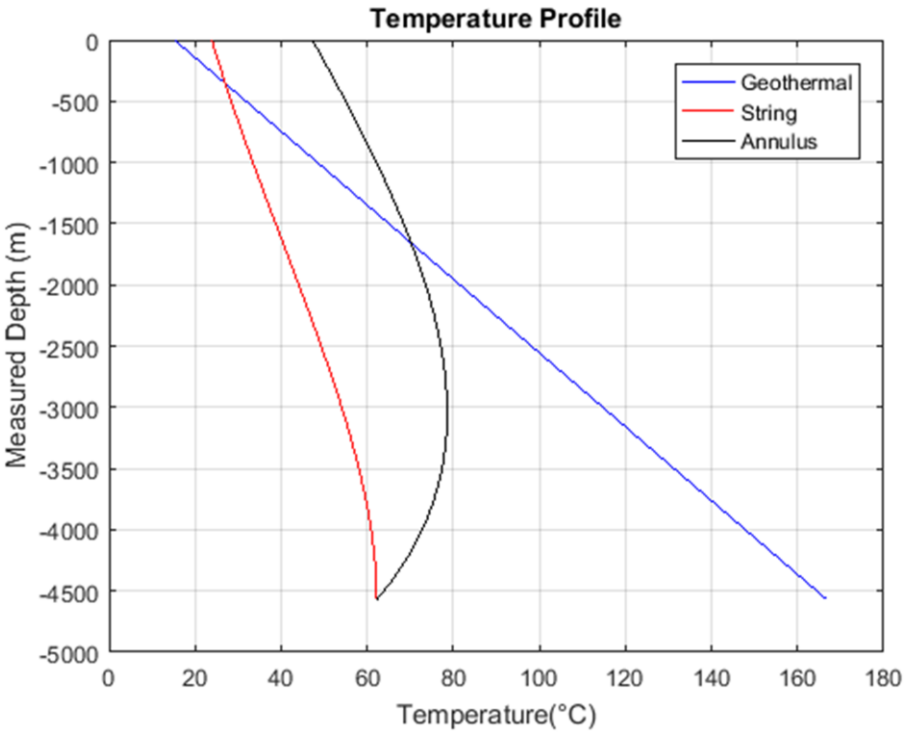

Fig 5. 20 Temperature distribution – geothermal gradient: 33.15 °C/km

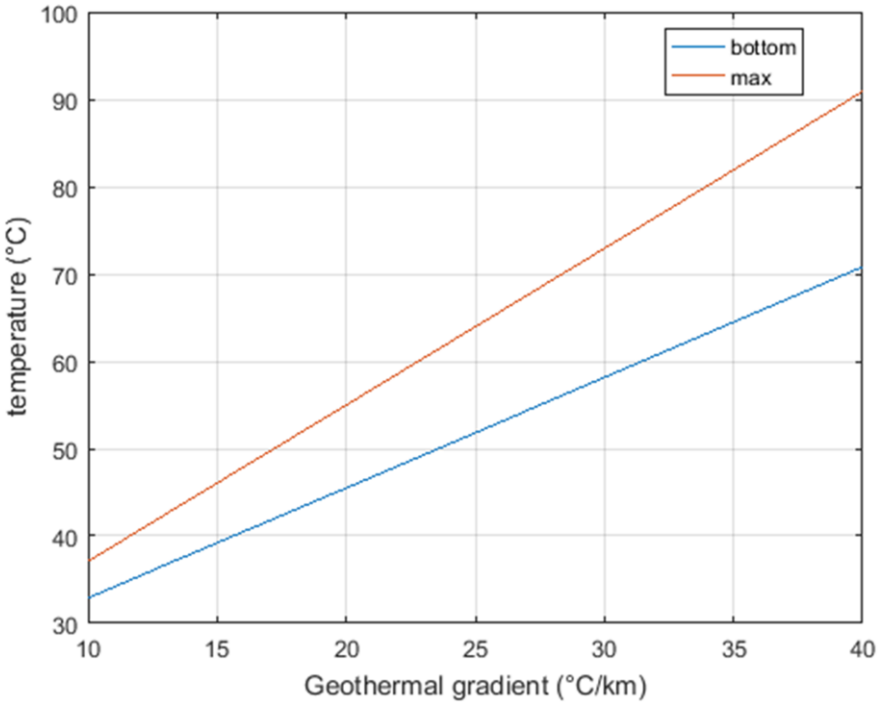

Fig 5. 21 Temperature vs. geothermal gradient

5.7. Energy source terms

Joule Thomson coefficient

The Joule-Thomson coefficient determines the change in drilling fluid temperature with changes in pressure. The wellbore pressure distribution will therefore have a direct impact on the temperature distribution.

Figure 5.22 gives a plot of bottom hole temperature versus flow rate for the base case without the Joule-Thomson effect and a the same case but the Joule-Thomson effect is included. The comparison reveals that the bottom hole temperature decreases when the effect of the Joule-Thomson coefficient is considered. This is because as pressure increases in the drill pipe with flow direction, the drilling fluid compresses and cools. For example for the case where the flow rate is set to 1500 l/min a reduction of bottom hole temperature by 3.6% is noticed.

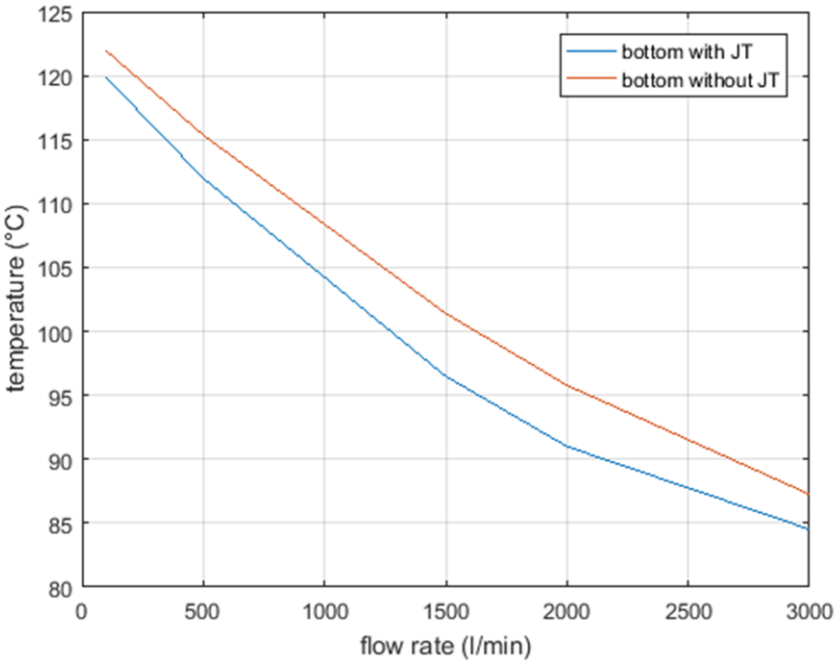

Fig 5. 22 Bottom hole temperature vs. flow rate

Frictional pressure losses

As explained in chapter 2, frictional pressure losses will introduce heat to the wellbore system. Simulations are performed using the base case with varying flow rates in the range of 500-3000 l/min with and without the effect of frictional pressure losses.

Figure 5.23 reveals that the effect is significant on the bottom hole temperature. At a flow rate of 3000 l/min where the effect is largest, the bottom hole temperature for the two scenarios differ by 48%. At a flow rate of 500 l/min where the effect is minimal, the bottom hole temperature for the two scenarios differ by 1%. Thus, heat generation from frictional pressure losses produce a great effect on the wellbore temperature distribution.

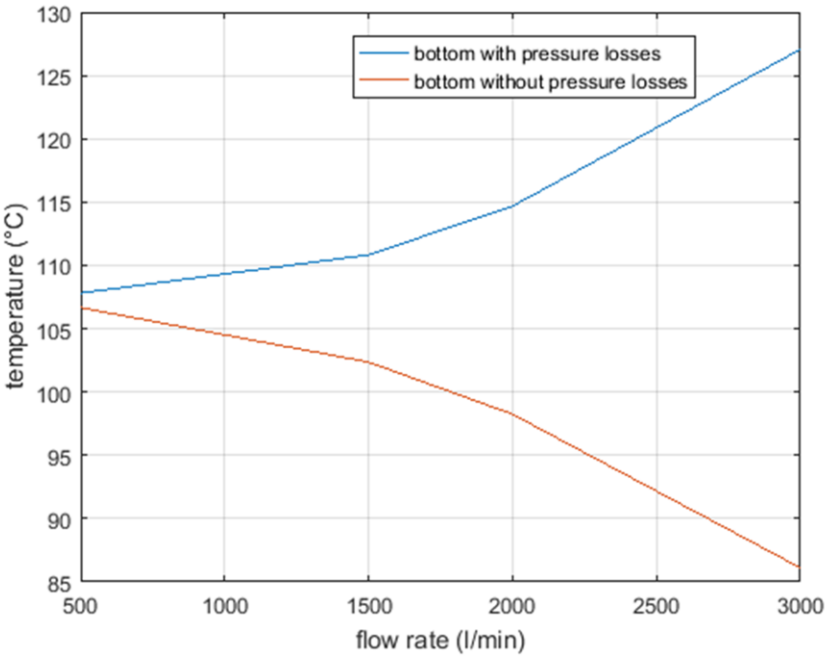

Fig 5. 23 Bottom hole temperature vs. flow rate

5.8. Effect of pressure and temperature on density and viscosity on temperature

Figure 5.24-25 represents temperature distribution with constant density and viscosity (continues curve) and with depending density and viscosity on temperature and pressure (Intermittent curve) with a flow rate of 300 l/min and 3000l/min respectively.

We conclude that it is very important to consider the density and the viscosity as a function of temperature and pressure because the simulations shows a great difference up to 20°C.

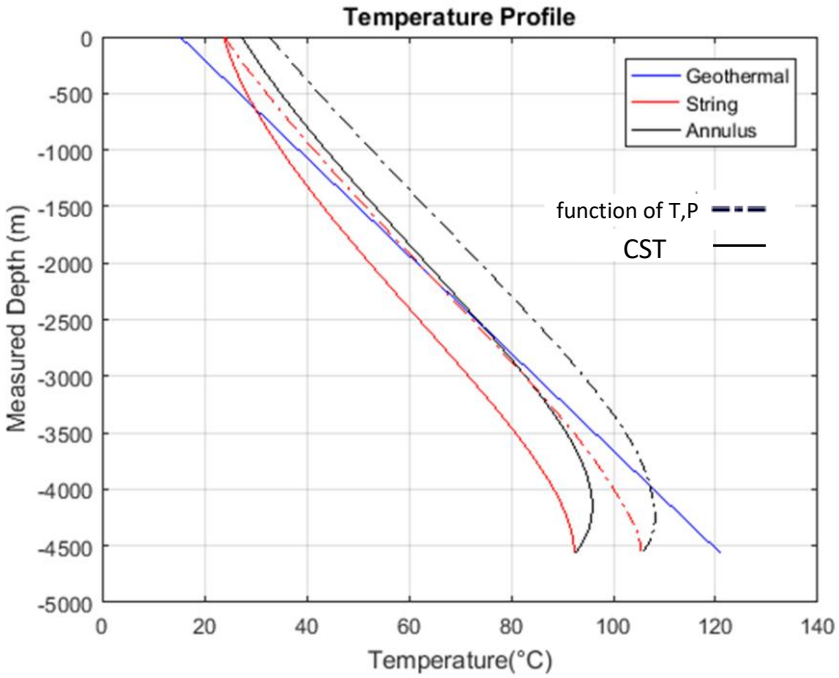

Fig 5.24 flow rate of 300 l/min

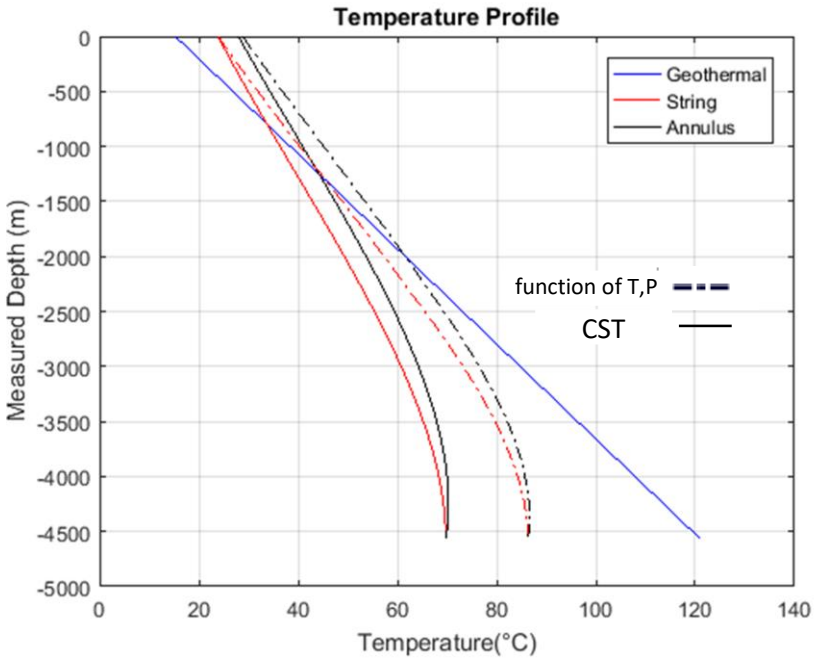

Fig 5. 25 flow rate of 3000 l/min

5.9. Circulation Time

The proposed model is a semi-transient model as it considers a transient heat transfer in the interface well formation, and a permanent heat transfer in the wellbore. Figure 5.26 shows the changes in temperature over time from 6 hours to 240 hours (10 days). Simulation shows a decrease in temperature over time, therefore the distribution of the temperature of the mud moves away from the temperature of formation over time which is very logical because if the circulation time is reduced the mud will not have the chance to cool down, On the other hand, the longer the circulation time is, the more mud will cool down.

We also notice that the temperature stabilizes over time; we are getting closer to the permanent regime.

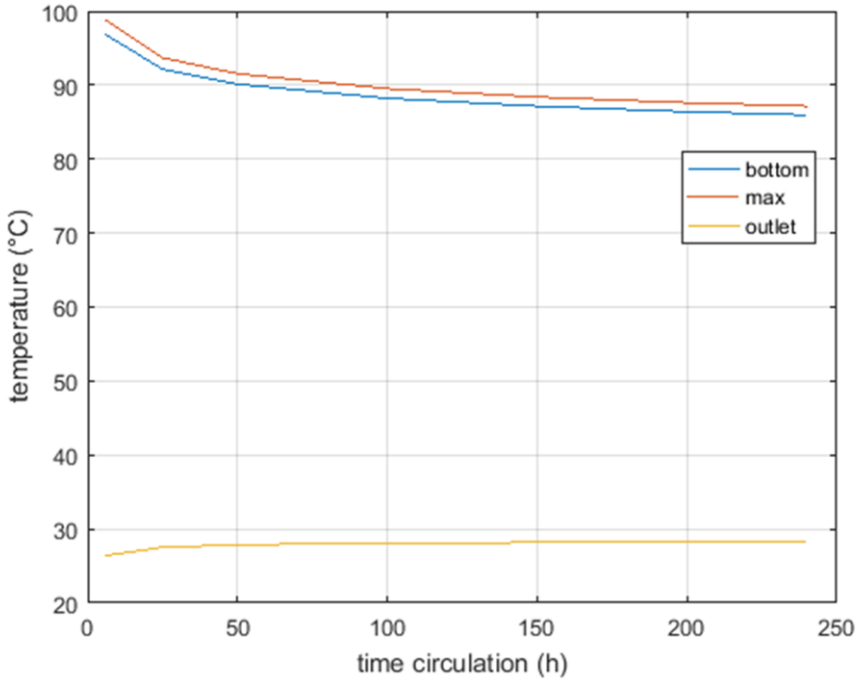

Fig 5. 26 temperature vs circulation time

5.10. Multi layers well

One of the advantages of our model is to calculate the temperature distribution in wells where the geometry is complicated, for example wells with several layers.

Figure 5.27 shows the diagram of half of the well which contains 4 layers. The purpose of using these layers is to strengthen the structure of the well and also to decrease the heat transfer from the formation to the well.

The comparison between the base case and this case shows a decrease in temperature of one degree Celsius as shown in figure 5.28.

Table 5.1 summarizes the dimensions of the diameters of the well in mm.

Table 5. 1 dimensions of the multi layers well

Well od 1	Casing1 od	Casing 1 id	Casing 2 od	Casing 2 id	Casing 3 od	Casing 3 id	Drill pipe wall od	Drill pipe wall id
660,4	473,075	431,8	330,2	304,8	228,6	203,2	152,4	127

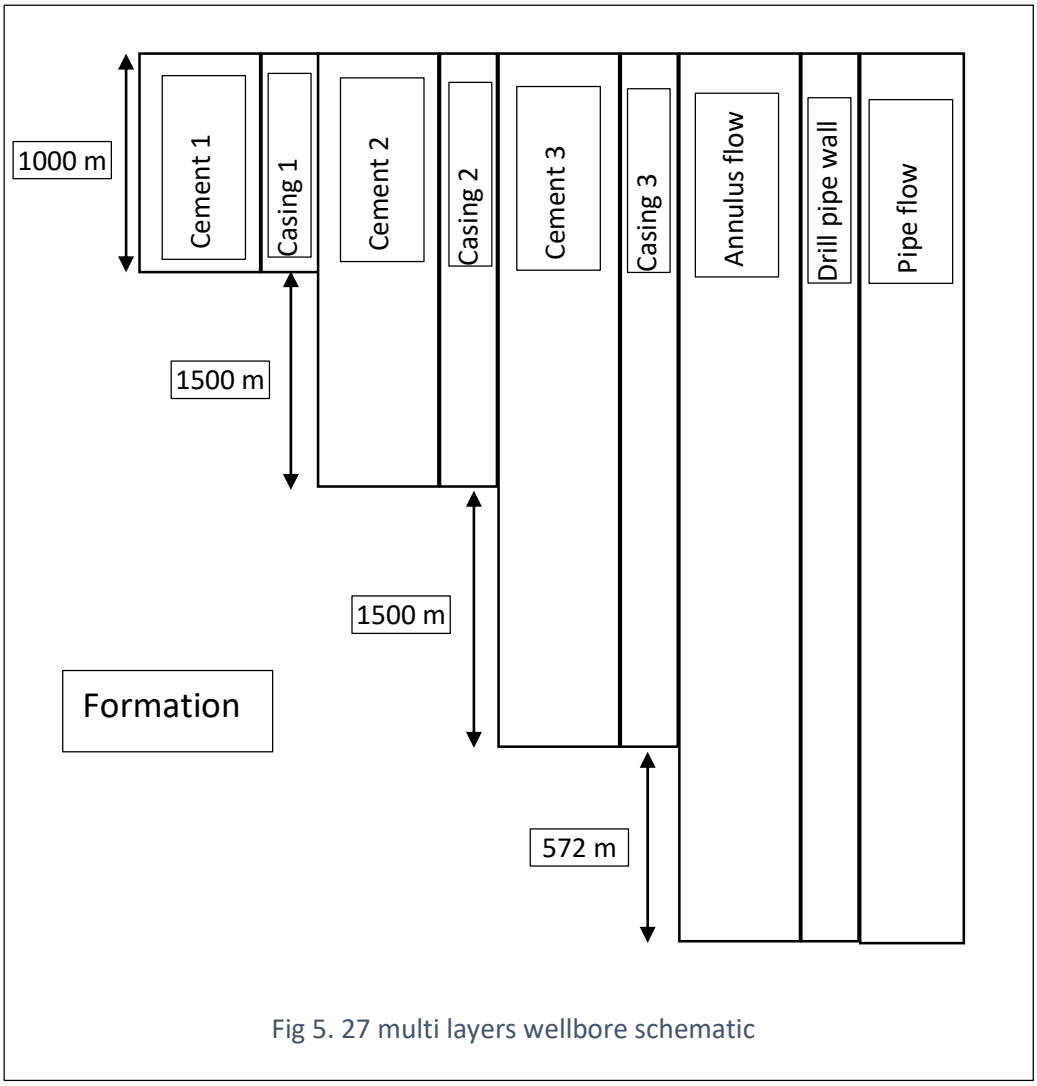

Fig 5. 27 multi layers wellbore schematic

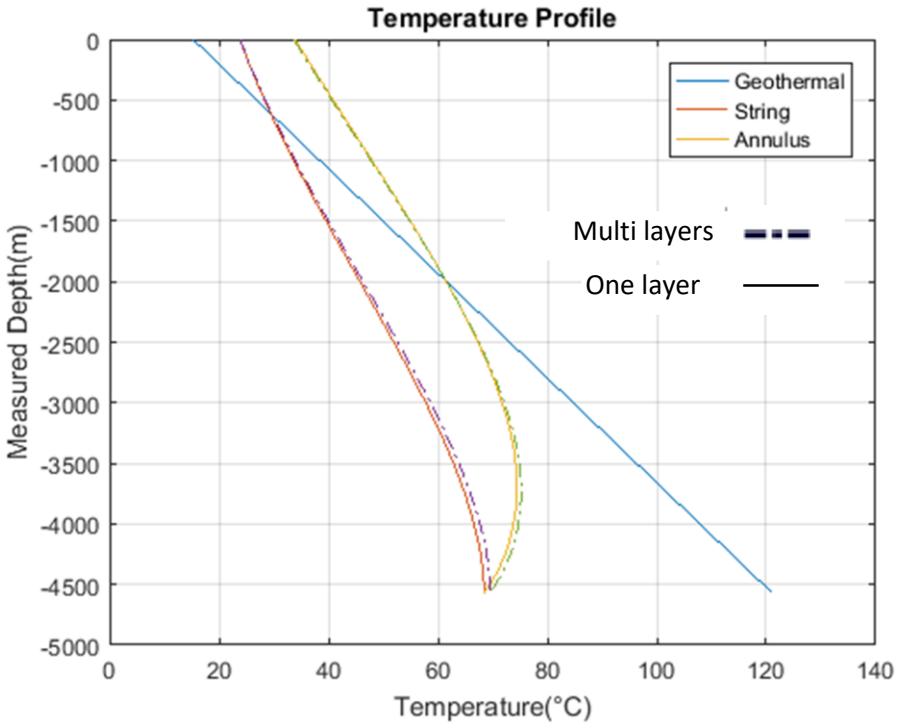

Fig 5. 28 compariason between a multi layer well and an open hole well

Conclusion

In this chapter a sensitivity analysis is performed, and the goal was to determine the parameters that affect the temperature distribution the most, and this will help us to ensure a safe and profitable drilling operations.

Analyzing the simulation results reveals that the flow and the drilling fluid properties are the dominant factors for the wellbore temperature distribution. Changes in flow rate, drilling fluid density, or specific heat capacity are found to have a large effect on the maximum and bottom hole temperatures. Increasing the flow rate or drilling fluid density results in reduced wellbore temperatures. The opposite effect but occurs while increasing the drilling fluid thermal conductivity.

The other parameter which has a significant effect is the geothermal gradient, results show that increasing the geothermal gradient will increase the wellbore temperature.

The effects of energy source terms that occur during drilling are also investigated. In general, results show that the overall contribution from these terms is also predominant.. Also, considering energy source terms will improve the accuracy of the temperature model and it is suggested that they are not neglected.

General conclusion

General conclusion

In this study, we set ourselves the objective of establishing a model for the calculation of the temperature distribution of a fluid during drilling. We have established the equations of heat transfer between the well and the formation and for the resolution of these equations we have proposed a numerical algorithm taking into account the boundary conditions.

The model is improved by considering the sources of energy and also by taking into account the dependence of the density and the viscosity of the pressure and the temperature. In order to be able to do that a numerical approach is employed.

The model proposed is a steady-state model so it can be improved by considering the transient effect.

The model is validated with the existing analytical models.

After the simulations, the parameters which influence the temperature of the fluid such as the flow rate have been specified to control the operation of the drilling.

The main fruit of this PFE project is the MATLAB software "WELL-TEMP" which is validated and ready to be consumed by the industrial field.

However, it is very important to validate the proposed model using real field data, object of future works.

References

References

[1] Bergman, Theodore L, Frank P Incropera, David P DeWitt, and Adrienne S Lavine Fundamentals of heat and mass transfer, 2011.

[2] Hasan, A. R., & Kabir, C. S. Heat Transfer During Two-Phase Flow in Wellbores; Part I-Formation Temperature. 1991.

[3] Kabir, C. S., Hasan, A. R., Kouba, G. E., & Ameen, M. Determining Circulating Fluid Temperature in Drilling, Workover, and Well Control Operations.1996

[4] Thompson, M., & Burgess, T. M. The Prediction of Interpretation of Downhole Mud Temperature While Drilling. 1985.

[5] E. Santoyo , A. Garcia , G. Espinosa ,Convective heat-transfer coefficients of non-Newtonian geothermal drilling fluids.

[6] Sharat V Chandrasekhar, P. V. Suryanarayana, B, Udaya. Circulating temperatures in complex wellbores.

[7] Kumar, A., & Samuel, R. Analytical Model To Predict the Effect of Pipe Friction on Downhole Fluid Temperatures. 2013.

[8] Aadnoy, B. S., Fazaelizadeh, M., and Hareland, G. A 3D analytical model for wellbore friction. Journal of Canadian Petroleum Technology, 2010.

[9] Hamrick, T. R. Optimization of Operating Parameters for Minimum Mechanical Specific Energy in Drilling: West Virginia University. 2011.

[10] Dan Sui, Vebjorn Haraldstad Langaker, Downhole Temperature Modeling for Non-Newtonian Fluids in ERD Wells.

[11] A. R. Hasan, C, S, Kabir. A Fluid Circulating Temperature Model for Workover Operations. 1996

[12] F.J. McQuillan, J.R. Culham and M.M. Yovanovich , Properties of dry air at one atmosphere.

[13] Charles S, Holmes, Samuel C, Swift. Calculation of Circulating Mud Temperatures, Journal Of Petroleum Technology.

[14] Al Saedi, A.Q., Flori, R.E., Kabir, C.S., New analytical solutions of wellbore fluid temperature profiles during drilling, circulating, and cementing operations, Journal of Petroleum Science and Engineering (2018).

Appendix

Appendix

Swift and Holmes model [13]

Basic Assumptions and Equations

The model is based upon the assumption that the heat transfer between the annular fluid and the formation can be approximated by steady-state linear heat transfer. Other simplifying assumptions are that the heat generated by the drill bit is negligible and that a linear geothermal profile exists.

The development of the model is depicted in Fig. 2.1. A slab of thickness dx is used, assuming heat transfer in the radial direction and no significant longitudinal conduction. The heat accumulation of the annular fluid between depth x and $x + dx$ is given by

$$Q_{a(x+dx)} - Q_{a(x)} = m_a c_{pa}\left(T_{a(x+dx)} - T_{a(x)}\right) \qquad (1)$$

And the steady-state approximation of the heat transferred between the annular fluid and the formation is given by

$$Q_f = 2\pi r U\left(T_a - T_f\right) \qquad (2)$$

The heat balance across the drill pipe is represented by:

$$Q_{ap} = 2\pi h_p r_p\left(T_p - T_a\right)dx \qquad (3)$$

Combining these equations yields the over-all heat transfer through the annulus.

$$mc_p.\frac{dT_a}{dx} + 2\pi r_p h_p\left(T_p - T_a\right) = 2\pi r U\left(T_a - T_f\right) \qquad (4)$$

The formation temperature may be approximated as:

$$T_f = T_s + Gx \qquad (5)$$

Substituting Eq. 5 into the over-all heat balance for the annulus produces the heat balance for the element across the armulus fluid:

$$mc_p.\frac{dT_a}{dx} + 2\pi r_p h_p\left(T_p - T_a\right) = 2\pi r U(T_a - T_s + Gx) \qquad (6)$$

A similar development for the fluid in the drillstem gives the following heat balance:

$$mc_p.\frac{dT_p}{dx} = 2\pi r_p h_p\left(T_p - T_a\right) \qquad (7)$$

These are the equations of the linear heat transfer model. The equations are then integrated into their applicable form. These are, for the temperature of the mud in the drillstem,

$$T_p = K_1 e^{C_1 x} + K_2 e^{C_2 x} + Gx + T_s - GA \qquad (8)$$

and for the temperature of the mud in the annulus

$$T_a = K_1 C_3 e^{C_1 x} + K_2 C_4 e^{C_2 x} + Gx + T_s \qquad (9)$$

Where

$$C_1 = \left(\frac{B}{2A}\right).\left[1 + \left(1 + \frac{4}{B}\right)^{1/2}\right]$$

$$C_2 = \left(\frac{B}{2A}\right).\left[1 - \left(1 + \frac{4}{B}\right)^{1/2}\right]$$

$$C_3 = 1 + \left(\frac{B}{2}\right).\left[1 + \left(1 + \frac{4}{B}\right)^{1/2}\right]$$

$$C_4 = 1 + \left(\frac{B}{2}\right).\left[1 - \left(1 + \frac{4}{B}\right)^{1/2}\right]$$

$$A = \frac{mc_p}{2\pi r_p h_p}$$

$$B = \frac{rU}{r_p h_p}$$

These equations when applied with the proper boundary conditions represent the analytical solution of the mud temperature profiles for the fluid in the drillstem and annulus.

Solution of Equations to Derive Circulating Mud Temperatures

Since the annular and drillstem mud temperatures are equal at the bottom of the well, the following boundary conditions may be applied to obtain the bottomhole temperature.

Boundary Condition 1 at $x = 0$; $T_p(0) = T_{pi}$

Boundary Condition 2 at $x = H$; $T_p(H) = T_a(H)$

For these boundary conditions the following integration constants are obtained:

$$K_1 = T_{pi} - K_2 - T_s + GA$$

$$K_2 = \frac{GA - (T_{pi} - T_s + GA)e^{C_1 H}(1 - C_3)}{e^{C_2 H}(1 - C_4) - e^{C_1 H}(1 - C_3)}$$

These integration constants are applied to Eqs. 8 and 9 in order to calculate the temperature at any point in the well during circulation.

Hasan and Kabir's Model [14]

This model involves energy balance between the formation and annulus, and the annulus to the drillpipe as presented in Fig. 2.1.

The energy balance for the steady-state condition for the forward circulation in the annulus is given by

$$Q_{a(x+dx)} - Q_{a(x)} = Q_{ap} - Q_f \qquad (10)$$

Where Q_f refer to the heat flow form the formation to the wellbore, which can be written as

$$Q_f = \frac{2\pi k_f}{T_D}(T_f - T_w)dx \qquad (11)$$

Then, the heat losses from the wellbore to the annulus can be calculated by the overall-heat-transfer coefficient of the annulus system as given by

$$Q = \frac{2\pi r_a U_a}{\mathrm{m}}(T_w - T_a)dx \qquad (12)$$

The amount of heat flow from formation to the wellbore is equal to the heat flow from wellbore to annulus; therefore, by eliminating T_w from Eqs. 11 and 12 we obtained the following expression:

$$Q_f = \frac{\mathrm{c_p} m}{\mathrm{A}}(T_f - T_a)dx \qquad (13)$$

Where

$$A = \frac{c_p m}{2\pi}.\left[\frac{(k_f + r_a U_a T_D)}{r_a U_a k_f}\right]$$

Then, Q_{ap} represent the heat losses from the annulus to the drilling string as

$$Q_{ap} = \frac{2\pi r_p U_p}{m}(T_a - T_p)dx \qquad (14)$$

Eq. 14 can be simplified as

$$Q_{ap} = \frac{c_p}{B}(T_a - T_p)dx \qquad (15)$$

Where

$$B = \frac{mc_p}{2\pi r_p U_p}$$

Substituting Eqs. 13 and 15 into Eq. 1 and simplifying, we obtained the following expressions for the annulus

$$A\frac{dT_a}{dx} = \frac{A}{B}\left(T_a - T_p\right) - (T_f - T_a) \qquad (16)$$

And for the drill-pipe

$$T_a = T_p + B.\frac{dT_p}{dx} \qquad (17)$$

Differentiating Eq. 17 with respect to depth, we obtain

$$\frac{dT_a}{dx} = \frac{dT_a}{dx} + B.\frac{d^2T_p}{dx^2} \qquad (18)$$

Substituting Eqs. 17 and 18 into Eq. 16 and simplifying, and considering $T_f = T_s + G.x$, we obtained the following expression:

$$AB.\frac{d^2T_p}{dx^2} - B\frac{dT_p}{dx} - T_p + T_s + Gx = 0 \qquad (19)$$

The solution of the second-order ordinary differential equation above is obtained by the summation of solution for homogenous (complementary) equation and the particular solution of the inhomogeneous equation. The result for the tubular temperature is given by

$$T_p = \lambda e^{\epsilon_1 x} + \delta e^{\epsilon_2 x} + Gx - BG + T_s \qquad (20)$$

Applying Eq 20 into Eq. 17, we get a mathematical form for the annular temperature, which is given by

$$T_a = (1 + \epsilon_1 B)\lambda e^{\epsilon_1 x} + (1 + \epsilon_2 B)\delta e^{\epsilon_2 x} + Gx + T_s \qquad (21)$$

Where

$$\epsilon_1 = \frac{1 + \sqrt{1 + \frac{4A}{B}}}{2A}$$

$$\epsilon_2 = \frac{1 - \sqrt{1 + \frac{4A}{B}}}{2A}$$

The constants λ and δ of Eqs. 20 and 21 can be found by applying the proper boundary conditions. For the forward circulation in a vertical wellbore, BC's can be applied at two points; that is, at surface and bottomhole.

Boundary Condition 1 at $x = 0\,; T_p(0) = T_{pi}$

Boundary Condition 2 at $x = H\,; T_p(H) = T_a(H)$

$$\lambda = \frac{\left(T_{pi} + BG - T_s\right)\epsilon_2 e^{\epsilon_2 H} + G}{\epsilon_2 e^{\epsilon_2 H} - \epsilon_1 e^{\epsilon_1 H}}$$

$$\delta = \frac{\left(T_{pi} + BG - T_s\right)\epsilon_2 e^{\epsilon_2 H} + G}{\epsilon_1 e^{\epsilon_1 H} - \epsilon_2 e^{\epsilon_2 H}}$$